

The mean state of the Leeuwin Current system between North West Cape and Cape Leeuwin

C Pattiaratchi & M Woo

School of Environmental Systems Engineering,
The University of Western Australia, Crawley, WA 6009

Manuscript received August 2008; accepted September 2009

Abstract

The circulation and water mass characteristics offshore Western Australia between North West Cape and Cape Leeuwin (21–35° S) are described using findings from past studies as well as additional field data. The circulation pattern in the study region is dominated by the Leeuwin current system, which includes three main currents: the Leeuwin current (LC), the Leeuwin undercurrent (LU), and shelf current systems consisting of the Capes and Ningaloo currents. Localised discharges of fresh water and high salinity water were present in the shelf regions offshore Perth and Shark Bay, respectively. Localised upwelling also affected the water masses in the Geelvink Channel. Eight water masses were identified as interleaving layers of salinity and dissolved oxygen concentrations: (i) low salinity tropical surface water (TSW); (ii) high salinity south Indian central water (SICW); (iii) high dissolved oxygen subantarctic mode water (SAMW); (iv) low salinity Antarctic intermediate water (AAIW); (v) low oxygen north-west Indian intermediate (NWII) water; (vi) low oxygen upper circumpolar deep water (UCDW); (vii) high salinity low circumpolar deep water (LCDW); and (viii) cold (< 2 °C), high oxygen Antarctic bottom water (AABW). The LC consisted of tropical surface water and south Indian central water. In the northern region of the study area (between North West Cape and the Abrolhos Islands), SICW was present as a subsurface salinity maximum beneath the TSW. Between 28 and 29.5° S, the depth of the 35.7 salinity contour decreased from ~150 m to the surface. South of 29.5° S, SICW was present at the surface. Along the continental slope, the LU was present beneath the LC at depths between 300 and 800 m, with its core (lowest oxygen level) at 450 m. The LU transported SAMW north while the wind drove the continental shelf currents. Southerly, upwelling-favourable winds pushed the LC farther offshore (a process known as Ekman transport), which forced cold, upwelling water onto the continental shelf. The Ningaloo current mainly consisted of TSW and extended north from Shark Bay to beyond North West Cape; the Capes current consisted of SICW and was present as a continuous current system on the continental shelf, extending north from Cape Leeuwin to Geraldton—a distance of some 750 km.

Keywords: Leeuwin Current, Leeuwin Undercurrent, Ningaloo Current, Capes Current, water masses, Western Australia.

Introduction

Globally, eastern ocean basins are highly productive ecosystems, which support high primary productivity and large pelagic finfish stocks. The exception to this rule, however, is off the west Australian coast, where, although the wind regime resembles that of other eastern ocean margins, the waters are oligotrophic. Thus the first studies of the physical oceanographic processes off the west Australian coast contrasted the circulation off Western Australia with that from other eastern ocean margins, which led to the discovery of the Leeuwin current. Later studies addressed the Leeuwin current system dynamics and revealed the Leeuwin current system consisted of three main currents: the Leeuwin current, the Leeuwin undercurrent, and shelf current systems consisting of the Ningaloo and Capes currents.

The main contributors to the knowledge of the physical oceanographic processes off the west Australian coast have been Andrews (1977, 1983), Cresswell and Golding (1980), Hamilton (1986), Smith *et al.* (1991),

Pearce and Walker (1991), Cresswell and Peterson (1993), Gersbach *et al.* (1999), Pearce and Pattiaratchi (1999), Fang and Morrow (2003), Feng *et al.* (2003, 2005), Morrow *et al.* (2003), Ridgway and Condie (2004), Fieux *et al.* (2005), Woo *et al.* (2006a, 2006b), Rennie *et al.* (2007), Meuleners *et al.* (2007), Woo and Pattiaratchi (2008), Batteen and Miller (2008).

The main surface and subsurface current systems (Figure 1) along the west Australian coast are:

- the West Australian current
- the Leeuwin current
- the Leeuwin undercurrent
- continental shelf current systems consisting of the Capes and Ningaloo currents
- Shark Bay outflow
- localised flow associated with topographic features, such as the Houtman Abrolhos Islands and the Perth Canyon.

Here we describe each of the above current systems and discuss the surface and subsurface water masses

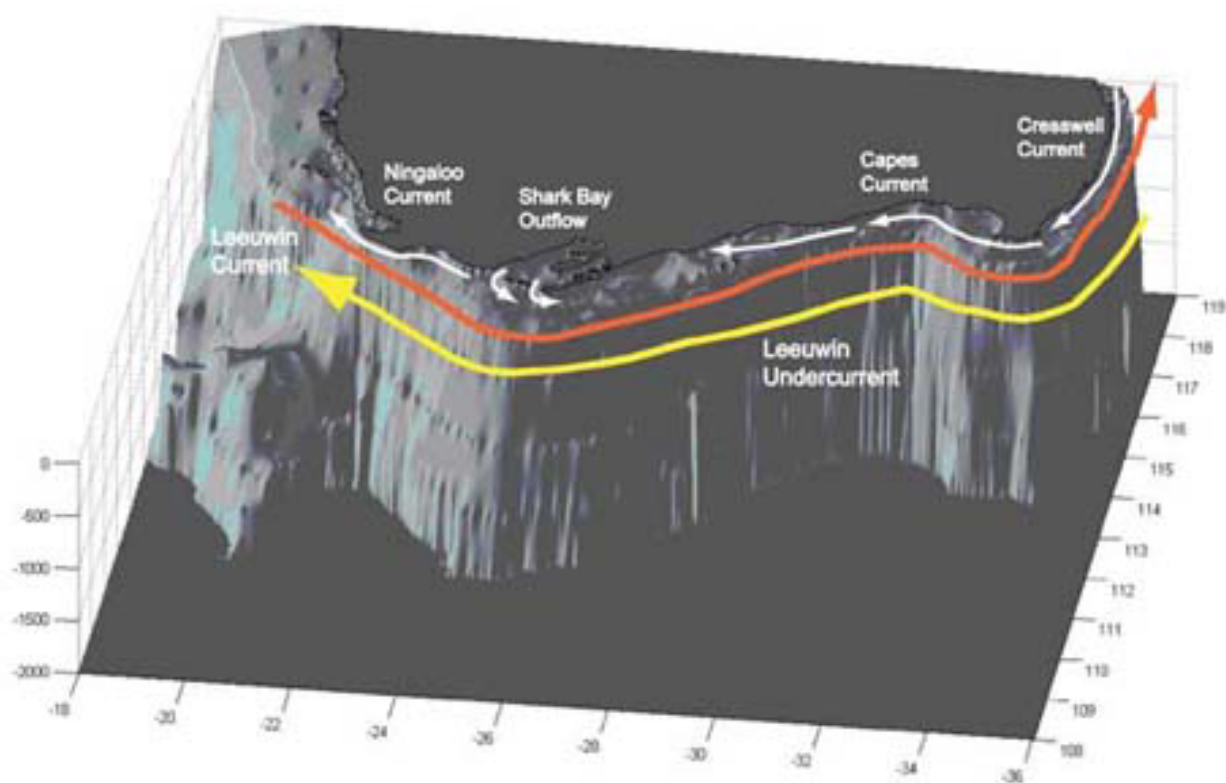


Figure 1. Schematic of the main surface and subsurface currents along the west Australian coast.

found in the study region. We also present data obtained from research voyages to the northern region (between North West Cape and the Abrolhos Islands) in November 2000 (ORV *Franklin* voyage no. 10/2000) and the southern region (between the Abrolhos Islands and Cape Leeuwin) in October/November 2003 (RV *Southern Surveyor* voyage no. 09/2003). Figure 2 shows the oceanographic station locations for both voyages.

Surface and subsurface currents

The West Australian current

Along most eastern ocean boundaries, equatorward eastern boundary currents are slower and wider than poleward western boundary currents and form one part of the anticyclonic subtropical gyre in each hemisphere's oceans. Sverdrup flow (the balance between wind stress, pressure gradients, and Coriolis acceleration) causes these gyres. Cool, upwelled water and high primary productivity, which supports the pelagic finfish industry, characterise eastern boundary current regions. The region offshore Western Australia does not have the same level of biological productivity as that induced by the Humboldt current off Peru or the Benguela current off Africa because the Leeuwin current (LC) suppresses the upwelling of cool, nutrient-rich water along the continental shelf (Pearce 1991).

The West Australian current is a shallow, equatorward surface current located farther offshore from the LC. It forms the eastern arm of the subtropical Indian Ocean gyre and its movement resembles the large, anticlockwise motion seen in southern ocean basins (Tomczak &

Godfrey 1994). Schott and McCreary (2001) proposed that the equatorward current was located a distance of more than 1000 km from the WA coast, and the width of it extended to 60°E.

Andrews (1977) suggested the West Australian current provided an eastward inflow of water to the LC at around 30–34° S and turned south near the coast between 29 and 31° S. Church *et al.* (1989) proposed the West Australian current turned south between 30 and 33° S and was entrained into the poleward LC flow. Cresswell and Peterson (1993) and Akhmer and Pattiaratchi (2006) suggested the inflow from the West Australian current strengthened the LC as the LC rounded Cape Leeuwin and turned into the Great Australian Bight.

The Leeuwin current

The circulation off the west Australian coast is different from that off other western continental margins (Schott 1935; Smith *et al.* 1991). In each of the main ocean basins, the surface circulation forms a gyre with a poleward flow along the western margin of the basin and a gyre with an equatorward flow along the eastern margin. The eastern margins (off south America and south Africa, for example) are also areas of high productivity due to upwelling, except off the west Australian coast where the LC transports water poleward (Figures 1 and 3).

The LC is a shallow (< 300-m-deep), narrow (< 100-km-wide) band of warm, low salinity, nutrient-depleted water of tropical origin, which flows poleward from Exmouth to Cape Leeuwin and into the Great Australian Bight (Church *et al.* 1989; Smith *et al.* 1991; Ridgway & Condie 2004). The LC signature extends from North West

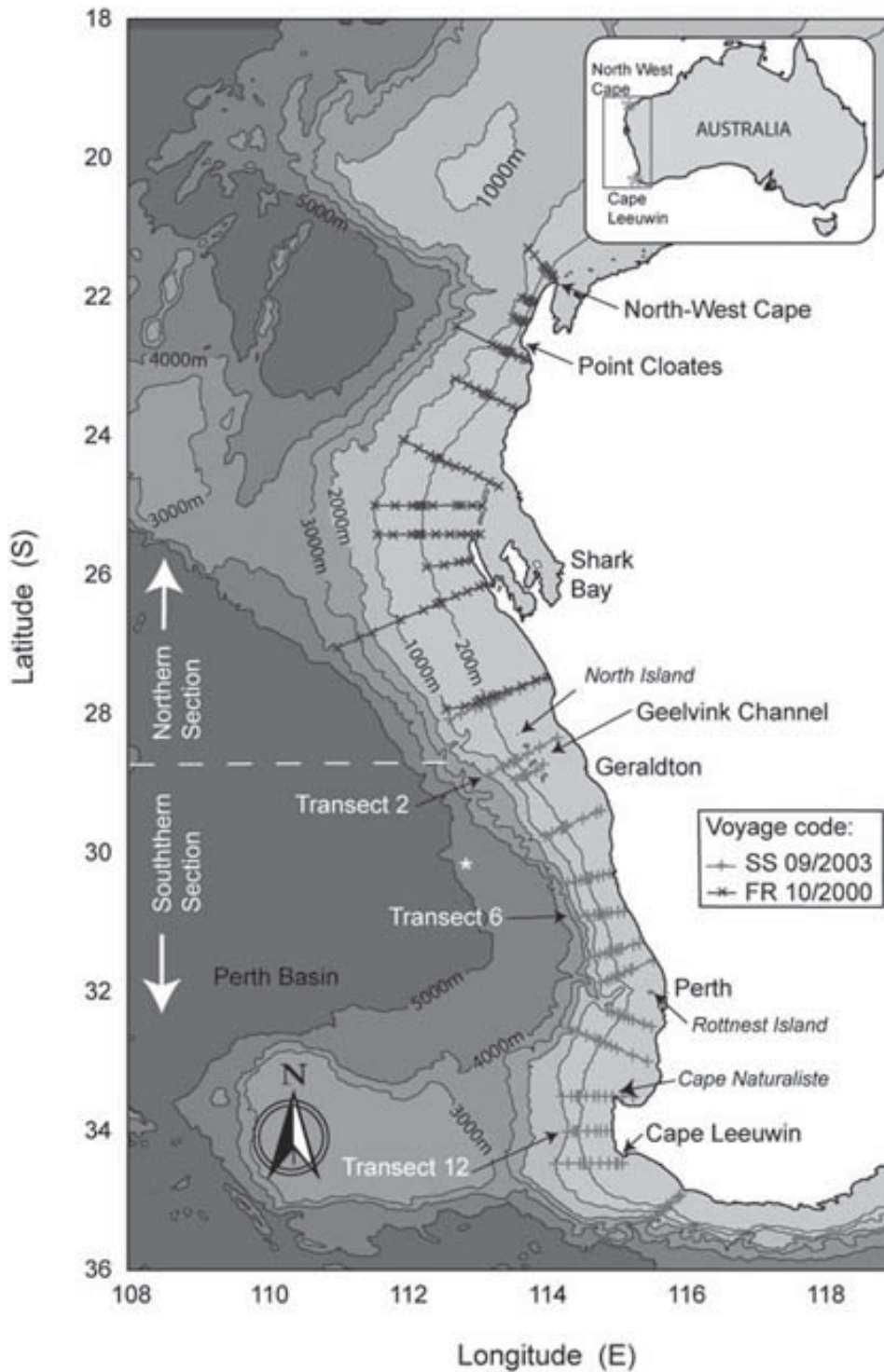


Figure 2. Bathymetry of the study region as well as the locations of the CTD transect lines and stations (from voyages SS09/2003 and FR10/2000), the meteorological stations (*italics*), and the deep water CTD station (*).

Cape to Tasmania as the longest boundary current in the world (Ridgway & Condie 2004). Cresswell and Peterson (1993), who defined the LC as a warm current of tropical origin, found that water from the West Australian Current increased the LC salinity in summer.

Warm, low salinity water from the Pacific Ocean, which flows through the Indonesian archipelago to the Indian Ocean, creates low density water (compared with

the cooler, saltier ocean waters off south-west Australia) in the region between Australia and Indonesia. The resulting density difference, which sets up a sea level gradient of about 0.5 m along the west Australian coast, is the LC's driving force. The earth's rotation causes water from the Indian Ocean to be entrained into the LC as the LC flows south; thus the LC strengthens as it flows south.

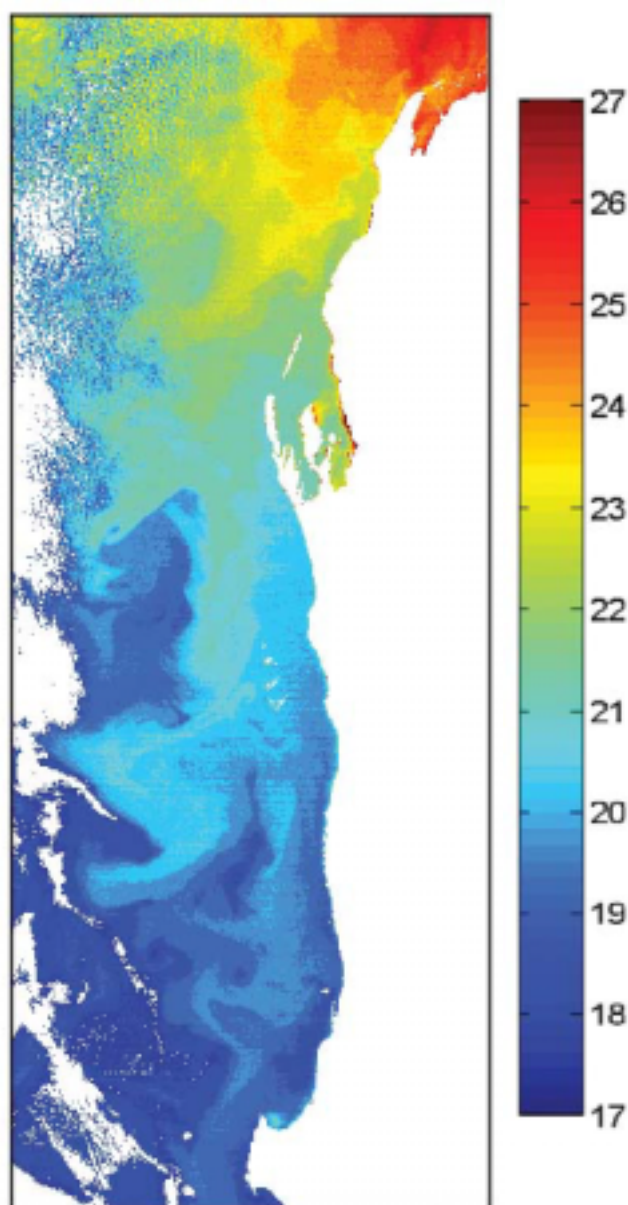


Figure 3. MODIS-derived satellite sea surface temperature image of the Leeuwin current obtained on 10 November 2007.

Studies have shown that along the west Australian coast, an alongshore pressure gradient, which overwhelms the opposing equatorward wind stress, drives the LC (Thompson 1984, 1987; Godfrey & Ridgway 1985; Weaver & Middleton 1989; Batteen & Rutherford 1990; Pattiaratchi & Buchan 1991). These studies found the alongshore pressure gradient of the sea surface slope was -4×10^{-7} (relative to the 300 dB). This pressure gradient overcomes the upwelling-favourable winds and induces an onshore surface flow, which causes downwelling at the coast. Woo & Pattiaratchi (2008) found that the alongshore geopotential gradient of the sea surface slope along the 1000-m isobath was -4×10^{-7} (from north to south) relative to the 300 dB level. Onshore geostrophic flow from the central Indian Ocean towards Western Australia occurs between about 15 and

35° S. Geostrophic inflow in the north (15–28° S) and tropical water from the North-west Shelf forms the LC's warm, low salinity core (Smith *et al.* 1991; Woo *et al.* 2006b; Woo & Pattiaratchi 2008). Meuleners *et al.*'s (2007) numerical modelling results confirmed that the mean annual transport across the LC at 30° S was 5.7 Sv ($\times 10^6 \text{ m}^3\text{s}^{-1}$), of which the northern boundary (at 26° S) contributed 3.60 Sv, or 63%. They estimated the inflow of water through the western boundary due to geostrophic balance at 2.1 Sv, or 37%, and found it varied meridionally.

The LC has a seasonal and inter-annual variability: it is usually stronger in winter and under La Niña conditions and weaker in summer and under El Niño conditions (Feng *et al.*, 2003). The LC transport is strongest near the shelf edge in late summer and early autumn, farther seaward in winter, when it carries around 5 Sv, and weakest in summer (~ 2 Sv). Its seasonal variability reflects changes in the local wind stress: the LC is weakest along the west Australian coast in summer as it accelerates into the maximum equatorward wind stress and strongest in winter because of the weak equatorward wind stress and the strong pressure gradient (Godfrey & Ridgway 1985). The LC is also weak in summer along the south Australian coast because the prevailing winds are from the east and south-east.

The Leeuwin undercurrent

Few studies have examined the Leeuwin undercurrent (LU); however, Thompson (1984, 1987), while studying the LC off the west Australian coast, observed the LU flowing beneath the LC (Figure 1). Thompson (1984) also found the LU transported 5 Sv of salty (> 35.8), oxygen-rich, nutrient-depleted water northward at $0.32\text{--}0.40 \text{ ms}^{-1}$. Current meter data from the Leeuwin Current Interdisciplinary Experiment (Smith *et al.* 1991) confirmed Thompson's (1987) findings and revealed the undercurrent was narrow and located adjacent to the continental slope between the 250 and 450-m depth contours.

Meuleners *et al.* (2007) used numerical modelling tests to show the LU had a maximum speed of 0.35 ms^{-1} (with a mean speed of 0.1 ms^{-1}) and consisted of meanders and eddies, which the more energetic LC induced. They found the LU core was located beneath the LC core at depths between 250 and 600 m, with the continental slope forming its eastern border. Meuleners *et al.* (2007) also found that the LU's northward transport increased as the water warmed and became saltier, which suggested that as the LU moved north, it entrained water from farther offshore in a similar way to the LC.

An equatorward geopotential gradient located at the depth of the undercurrent drives the LU (Thompson 1984). Geopotential anomaly values taken from 500 dB/3000 dB (Wyrtki 1971) and 450 dB/1300 dB (Godfrey & Ridgway 1985) revealed the LU's presence; Thompson (1984) and Smith *et al.* (1991) also recorded subsurface slopes of 0.4×10^{-7} and 0.2×10^{-7} , respectively. Woo and Pattiaratchi (2008) used field data obtained from a section along the 1000 m contour, parallel to the west Australian coast, to estimate a slope of 1×10^{-7} , which was the LU's equatorward driving force enhanced by an east-west subsurface slope generated by the downwelling of the

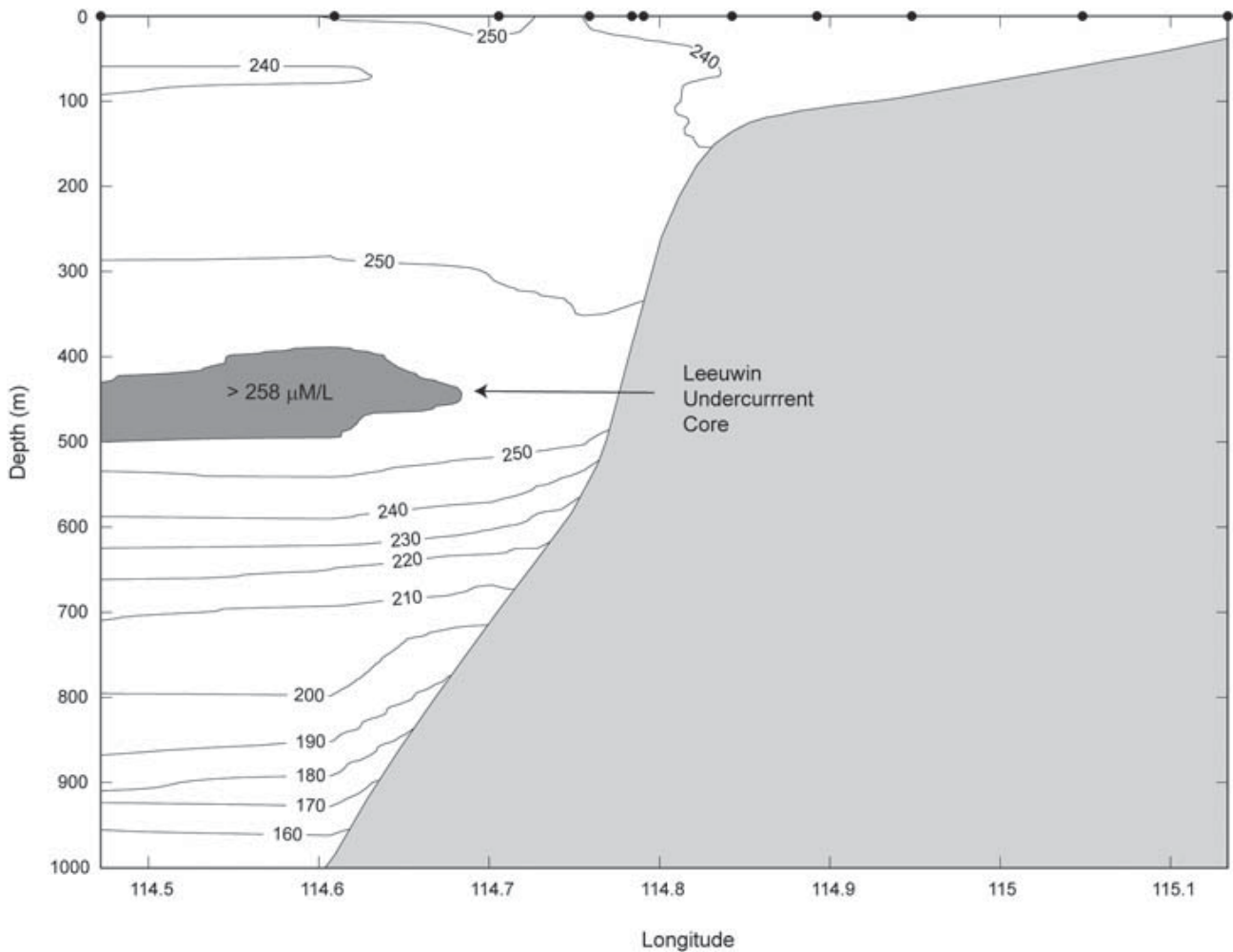


Figure 4. Cross-section of the dissolved oxygen levels for transect 6 showing the presence of the > 258 - $\mu\text{M/L}$ Leeuwin undercurrent core at 450-m depth. The transect location is shown in Figure 3.

LC. Meuleners *et al.* (2007) used numerical modelling tests to estimate a geopotential gradient of 1.9×10^{-7} acting towards the equator. All the gradients listed above are a factor of 10 less than the geopotential gradient associated with the surface LC.

The LU is also associated with the subantarctic mode water (SAMW). High convection in the region to the south of Australia results in cooling which is the generation mechanism for this water mass. As it has been formed recently ('age' of the water mass is small) it has a high dissolved oxygen concentration. A cross-section of the LU core was identified from the dissolved oxygen distribution: the core of the current consisted of a dissolved oxygen maximum of 252 $\mu\text{M/L}$ centred at a depth of about 450 m (Figure 4).

Several studies have shown the LU could be considered an extension of the Flinders current, which flows along the southern coast of Australian (Cirano & Middleton 2004; Akhir & Pattiaratchi 2006; Meuleners *et al.* 2007). The Flinders current is the dominant feature along the south Australian coast and extends from Tasmania to Cape Leeuwin (Cirano & Middleton 2004).

A positive (anti-clockwise) wind stress curl drives the Flinders current in summer and winter, which results in northward transport (due to Sverdrup balance) centred along 135° E, which is deflected to the west to satisfy vorticity dissipation and mass conservation (Cirano & Middleton 2004).

The Flinders current is present in summer and winter, but its westward transport, which occurs between 37 and 39° S and varies between 8 and 17 Sv, is stronger during the summer (Middleton & Bye 2007). The current, which extends through the water column to a maximum depth of 800 m and reaches maximum speeds of 0.5 ms^{-1} , offshore of the shelf break, interacts with the LC at the shelf break and slope. Here, the LC is visible as an eastward flowing surface current, with the Flinders current as the westward flowing subsurface current. Comparison of Akhir and Pattiaratchi's (2006) and Meuleners *et al.*'s (2007) temperature and salinity data obtained along the south and west Australian coasts showed the Flinders current sourcing the LU core.

Because the LU is linked to the Flinders current, its seasonal and interannual variability resembles that of the

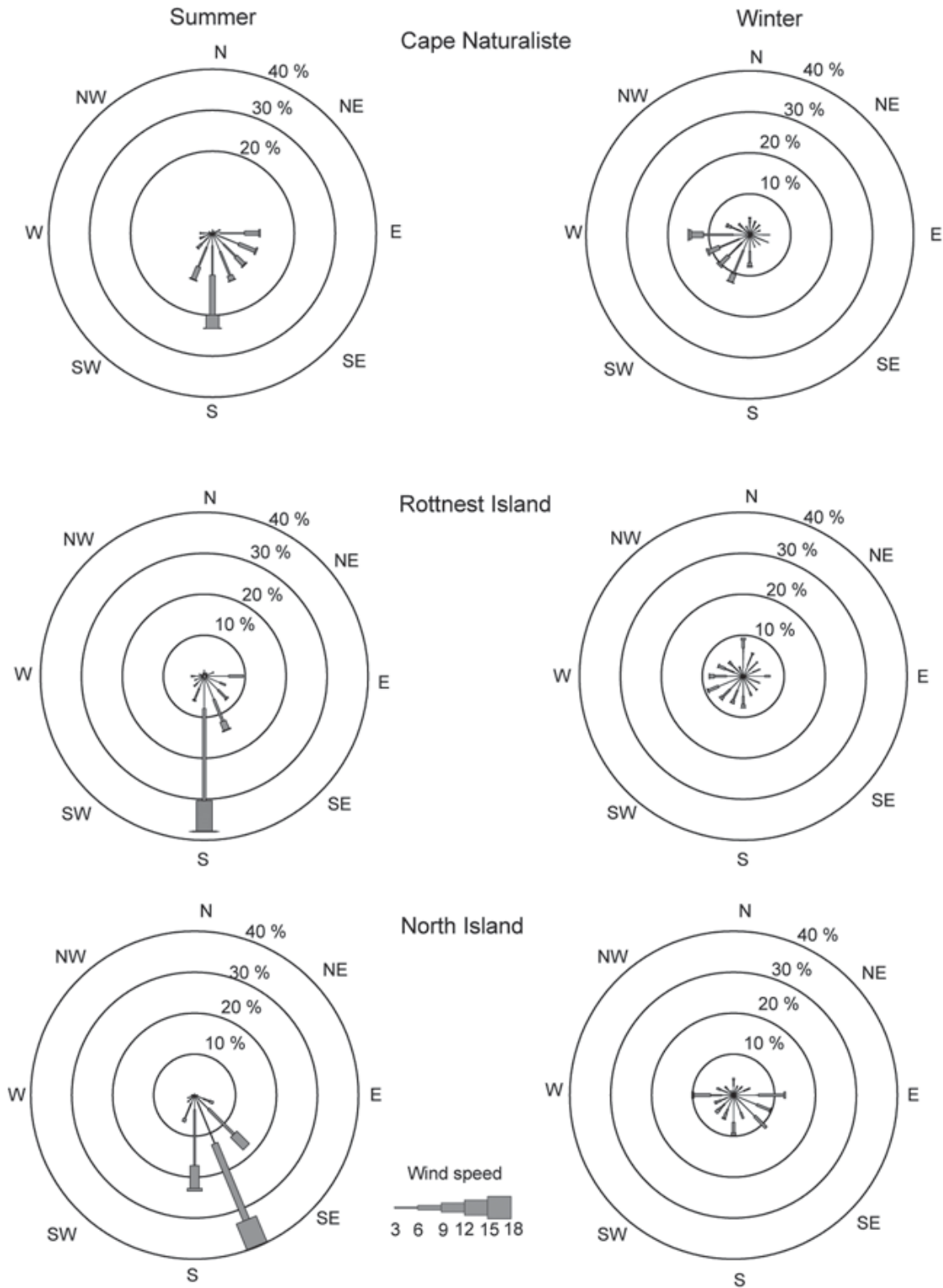


Figure 5. Summer and winter wind roses obtained from meteorological stations along the west Australian coast: Cape Naturaliste, Rottne Island, and North Island. The station locations are shown in Figure 3.

Flinders current. Thompson (1984) and Smith *et al.* (1991) used field tests to show the LU was strongest in summer between November and January. The Flinders current is also stronger during El Niño events; thus the LU would also be stronger during El Niño events.

Continental shelf currents

Several studies have used field data and satellite imagery to examine the continental shelf circulation along the west coast of Australia in summer (Cresswell *et al.* 1989; Cresswell & Peterson 1993; Pearce & Pattiaratchi

1997, 1999; Gersbach *et al.* 1999; Hanson *et al.* 2005a, 2005b; Woo *et al.* 2006a, 2006b). These studies found a cool, northward current (the Capes and Ningaloo currents) on the continental shelf, with the southward flowing LC usually located farther offshore.

Because wind drives the continental shelf currents, the seasonal variation in the wind field off Western Australia affects the currents' behaviour. Anticyclonic high pressure systems, as well as periodic tropic and extratropical cyclones (mid-latitude depressions) and seasonal sea breezes, dominate the weather systems around south-west Australia (Eliot & Clarke 1986). Eastward moving anticyclones pass the west coast every 3 to 10 days, with the anticyclonic band migrating from $\sim 38^\circ$ S in summer (mainly causing offshore winds) to $\sim 30^\circ$ S in winter (mainly causing onshore winds) (Gentili 1972). This seasonal movement of high pressure systems creates a strong seasonality in the wind regime along the west coast (Figure 5). In the summer, southerly winds prevail along the west coast. During the passage of a frontal system, the region is subject to strong winds (up to $25\text{--}30\text{ ms}^{-1}$) from the north-west, which change direction to the west then south-west over 12–16 hours; hence there is no dominant wind direction in winter. Up to 30 storm events may occur in any given year (Lemm *et al.* 1999).

In summer, the anticyclonic belt's southerly location causes an easterly airflow over Australia. This hot airflow forms a low pressure trough in a north-south (shore-parallel) direction (Kepert & Smith 1992). This pressure

trough, which is usually located inland, produces the prevailing southerly winds on the west Australian coast.

The combination of the sea breeze (south-westerly airflow) and the synoptic conditions (south-easterly airflow) causes a southerly sea breeze, which blows parallel to the shore, unlike the 'classic' sea breeze where the winds blow perpendicular to the shore. The sea breeze onset is rapid, with initially high velocities, and the surface currents respond almost instantly (Pattiaratchi *et al.* 1997). Masselink and Pattiaratchi (2001) examined wind fields at meteorological stations along the west Australian coast over a 40-year period. They found that about 200 sea breezes occurred annually, with wind speeds in the summer often exceeding 10 ms^{-1} . These strong, southerly winds dominated the continental shelf region in summer and drove the Capes and Ningaloo currents.

The Capes current

Seasonal flow reversals on the continental shelf offshore Rottnest Island was first reported by Rochford (1969) through the examination of annual salinity cycle and through the use of drift cards. Rochford (1969) found that there was a northward drift of higher salinity water during the summer months. Pearce and Pattiaratchi (1999) defined the Capes current as a cool, inner shelf current, which originated from the region between Capes Leeuwin and Naturaliste (i.e. 34° S) and moved equatorward along the south-west Australian coast in summer (Figure 6). Woo *et al.* (2006b) used field data to

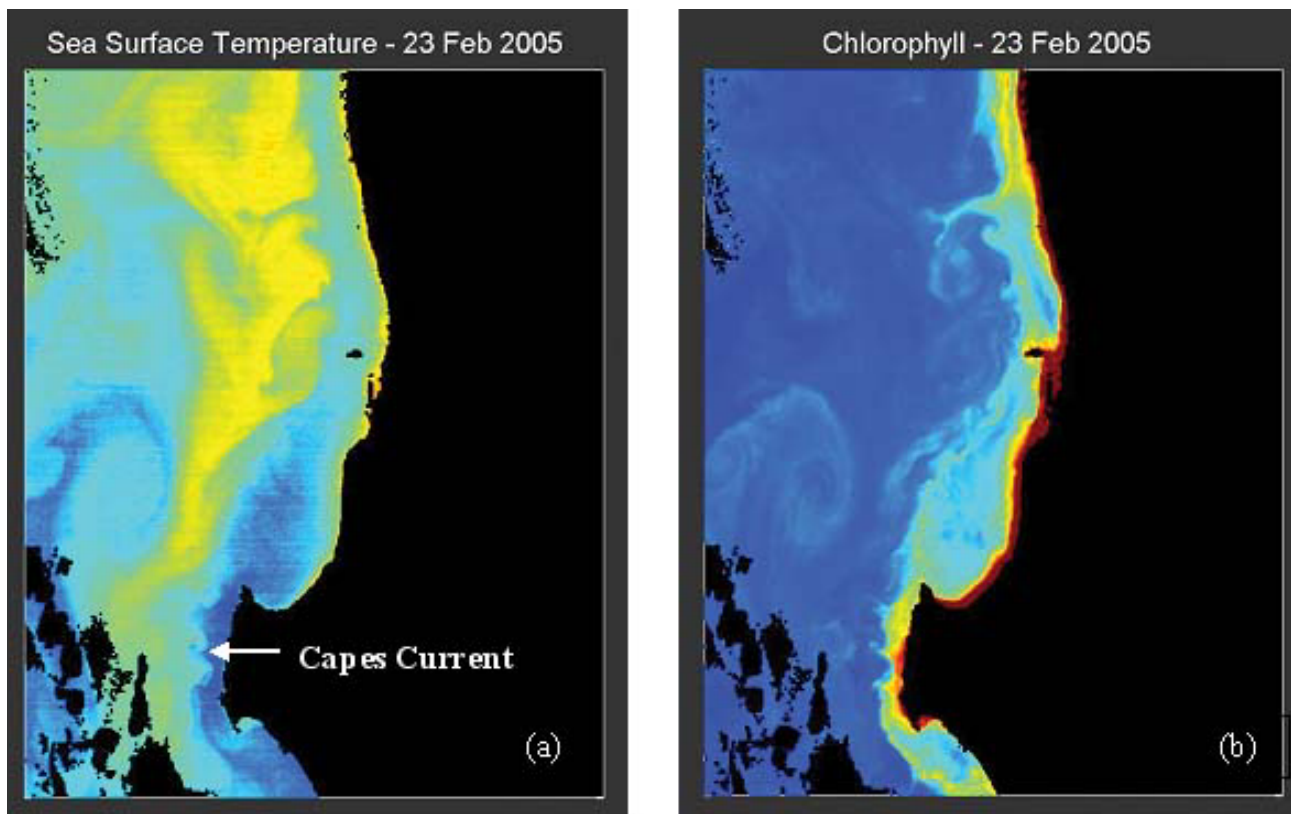


Figure 6. Ocean colour satellite images of the region offshore south-west Australia obtained with the MODIS (moderate resolution imaging spectroradiometer) on 23 February 2005 showing the sea surface temperature and the upwelling of cold water into the Capes current (a) and the associated high chlorophyll concentration (b).

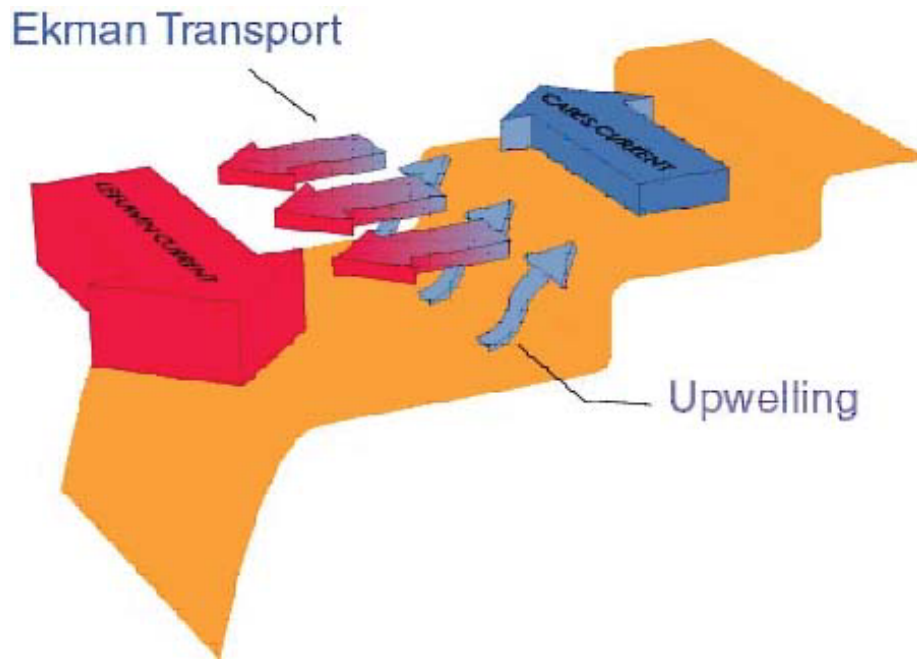


Figure 7. Cross-sectional schematic of the steady-state current regime off south-west Australia in summer (from Gersbach *et al.* 1999).

Sea Surface Temperature - 19 January 2007

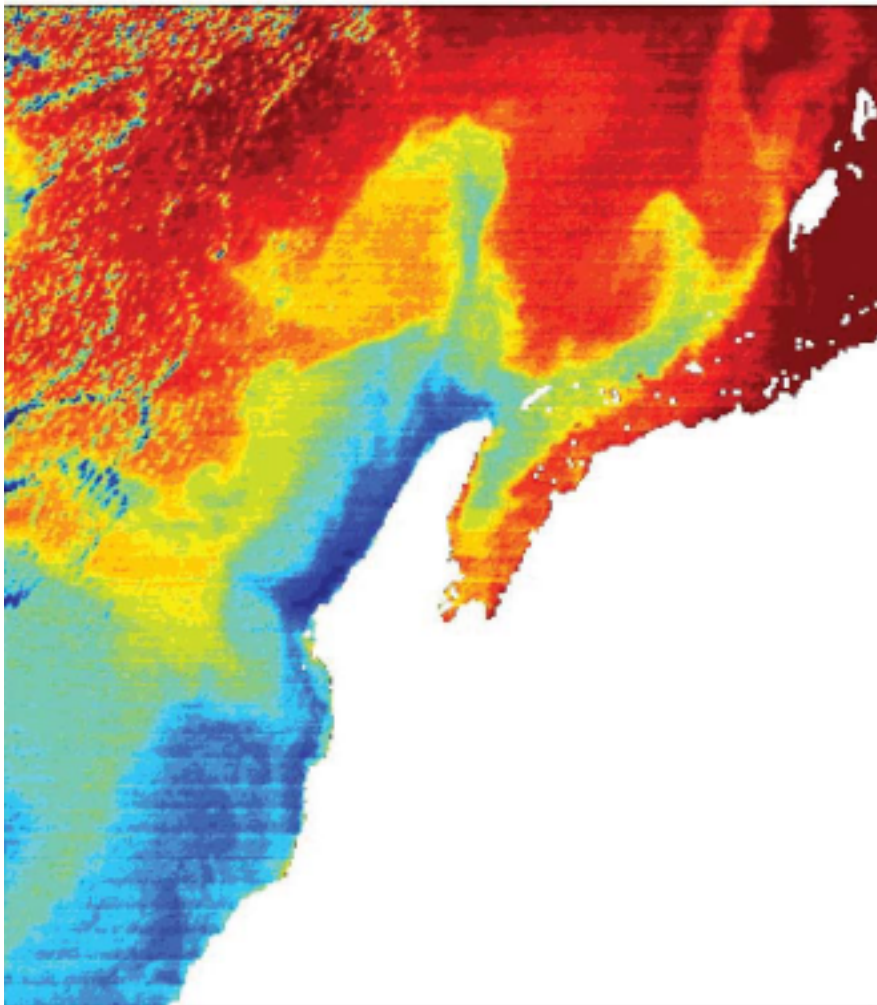


Figure 8. MODIS-derived satellite sea surface temperature image of the Ningaloo current obtained on 19 January 2007.

confirm the Capes current extended as far north as the Abrolhos Islands (32° S). The current has a salinity content of 35.37–35.53 and a temperature of 21.0–21.4 $^{\circ}$ C, which is cooler than the LC.

Several studies have found the Capes current is sourced from water upwelled from the bottom of the LC (at ~ 100 -m depth), which usually occurs between Capes Leeuwin and Naturaliste, and also from water from the south (to the east of Cape Leeuwin) (Gersbach *et al.* 1999; Pearce & Pattiaratchi 1999; Hanson *et al.* 2005a). The Capes current is well established by November when the winds in the region are mainly southerly because of the strong sea breezes (Pattiaratchi *et al.* 1997) and continues until about March when the sea breezes weaken.

Gersbach *et al.* (1999) described the dynamics of the Capes current off Cape Mentelle in their study on upwelling along the south-west Australian coast. Here the southerly wind stress overcame the alongshore pressure gradient, which pushed the surface waters and the LC farther offshore and upwelled cold water onto the continental shelf (Figure 7). Gersbach *et al.* (1999) also used numerical modelling to show that a wind speed of 8 ms^{-1} was enough to overcome the alongshore pressure gradient on the inner continental shelf.

The Ningaloo current

The Ningaloo current flows north along the inner continental shelf between the LC and the coast. A strong, southerly wind stress drives the current (Taylor & Pearce 1999; Woo *et al.* 2006a), similar to the Capes current along the south-west Australian coast. Taylor and Pearce (1999) used aerial surveys and satellite imagery to observe the Ningaloo current moving north along the Ningaloo reef front, forming a distinct line in the water and separating the coastal waters from the southward flowing LC some 2 km offshore. Studies using field data (Hanson *et al.* 2005b; Woo *et al.* 2006b) and numerical modelling (Woo *et al.* 2006a) found the Ningaloo current inshore of the 50-m isobath, extending from Shark Bay (Figure 2) to North West Cape and beyond.

At Point Cloates (Figure 2), under low wind conditions, the current splits and forms an anticyclonic

circulation pattern to the south-west (Figure 8; part of the current moves across the shelf to flow south, parallel to the coast. The LC water is taken northward adjacent to the Ningaloo reef, in the Ningaloo Current (Woo *et al.* 2006a). Woo *et al.*'s (2006b) field data showed the Ningaloo current consisted of colder ($< 23^{\circ}$ C), more saline (34.92) water than the offshore waters and had a similar temperature–salinity signature to the LC. Hanson *et al.* (2005a) recorded upsloping isotherms in their temperature contour plots of the region off south-west Australia, which showed upwelling had occurred off North West Cape. They also found the Ningaloo current had high nutrient concentrations and phytoplankton biomass and maximum regional primary production rates.

Shark Bay outflow

Shark Bay is a coastal, semi-enclosed embayment with deep, open waters to the north and two shallow gulfs to the south, bounded by three large islands to the west (Figure 2). Nahas *et al.* (2005) found a two-layered flow of seawater in the Geographe and Naturaliste channels, with the less dense, low salinity water flowing into the bay at the surface and the high density, high salinity water exiting the Bay near the seabed (Figure 9). James *et al.* (1999) proposed that a plume of high salinity water flowed south on the continental shelf near the seabed. Woo *et al.* (2006b) used a temperature–salinity diagram to show the outflow water had a high salinity. We identified the high salinity water from Shark Bay as a distinct water mass on the continental shelf with a temperature ranging between 21.2 and 22.9 $^{\circ}$ C and salinity up to 36.1.

Localised flow associated with topographic features: the Perth Canyon

The interaction between shelf and slope current systems causes localised flow patterns, which affect the ecology in the canyon vicinity. Compared with their surroundings, submarine canyons have higher biodiversity and biological productivity (Hickey 1995), which is often attributed to upwelling at the canyon

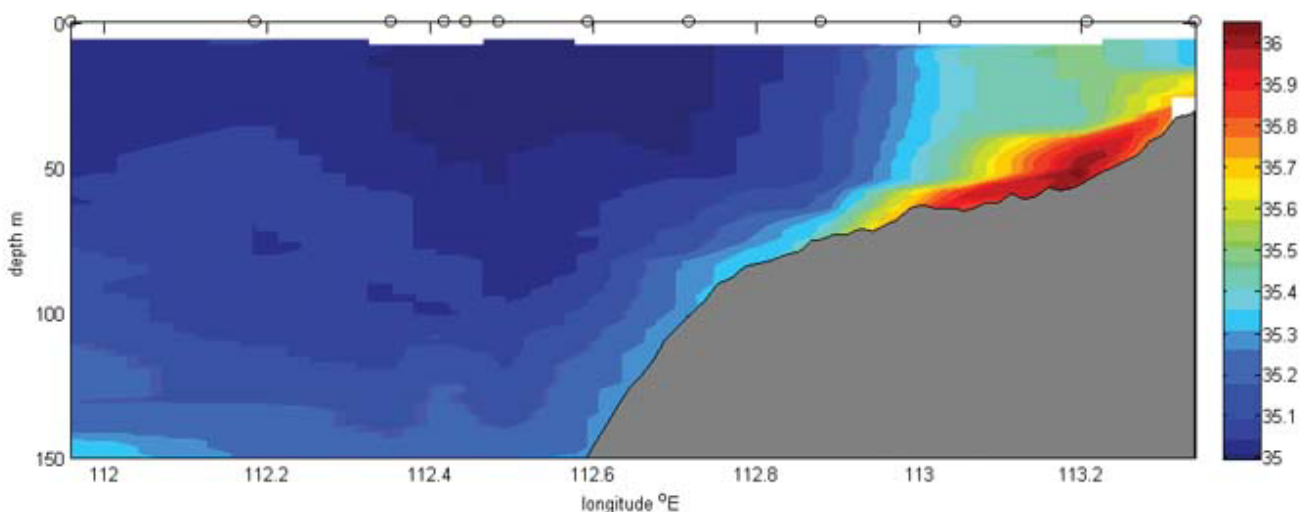


Figure 9. Cross-sectional transect of the region offshore Shark Bay showing the high salinity outflow of water onto the continental shelf.

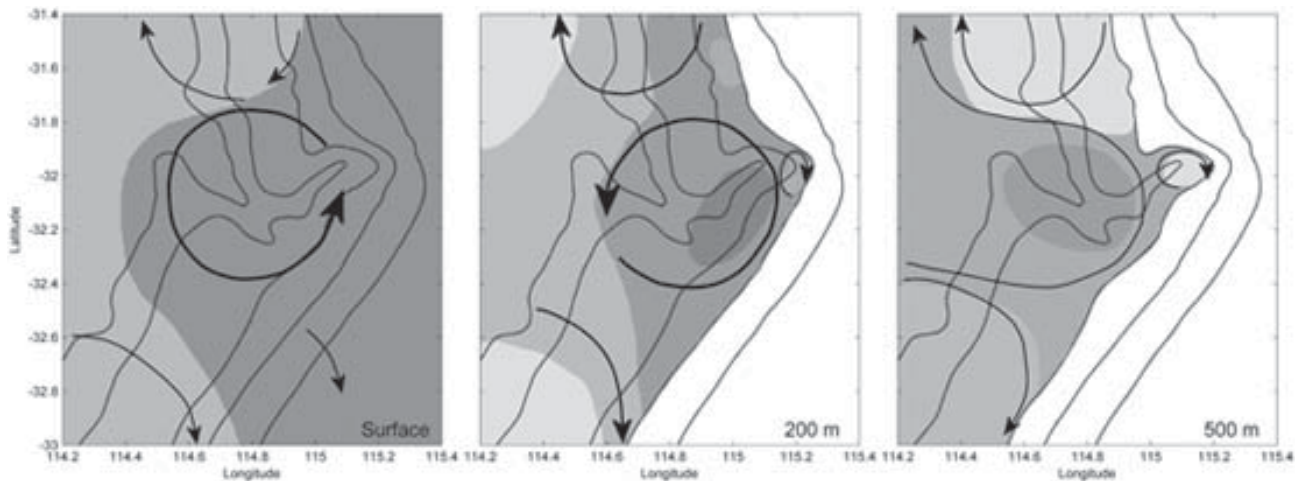


Figure 10. Water flow patterns in the Perth Canyon at the surface, 200-m, and 500-m depths. The shading indicates the temperature, with the lighter shades (colder temperature) showing the upwelling regions (from Rennie *et al.* 2009).

enriching the photic zone with nutrients. The Perth Canyon is an extension of the Swan River system within the Mentelle sub-basin, which cuts into the continental shelf west of Perth and Rottnest Island. The canyon starts at the 50-m contour and is ~100-km long and ~10-km wide near its head. It is 3-km-deep at the shelf slope and cuts 4-km-deep into the continental slope. At the canyon head, the depth plunges from 200 to 1000 m, with the canyon mouth opening onto the abyssal plain at a depth of 4000 m. Hence the Perth Canyon can be described as long, deep, narrow, steep-sided and intruding into the continental shelf.

Rennie *et al.* (2009) found that the LU interacting with the canyon generated eddies within the canyon (Figure 10). These clockwise eddies, which were formed over five to ten days and favoured upwelling at their centre, would then migrate farther offshore. Eddies sometimes recurred within the canyon, which suggested the canyon regulated the circulation, with several circular eddies of different sizes and depths present in the canyon at any given time. These circulation patterns enabled the canyon to support high levels of primary and secondary production; indeed the canyon was a feeding area for pygmy blue whales during the summer (Rennie *et al.* 2006).

Eddies caused regions of upwelling or downwelling, with deep upwelling stronger in the canyon than elsewhere on the shelf. Near-surface vertical transport was strong everywhere when wind forcing was present.

The circulation in the canyon produced upwelling to above 300-m depth, mainly at the head and along the canyon rims, but also contributed to downwelling. Rennie *et al.*'s (2007) model results suggested upwelling at the canyon head occurred when a clockwise surface eddy was centred over the south rim, whereas an eddy (either clockwise or anticlockwise) centred on the north rim caused net downwelling.

Increased upwelling, combined with strong, upwelling-favourable winds and the entrainment of eddies within the canyon, increased the primary productivity in the canyon; however, the LC formed a strong barrier to water upwelling to the surface. Because the canyon rims are deep, upwelling alone was insufficient to transport nutrients to the euphotic zone.

Surface and subsurface water masses

Temperature data from bathythermographs and CTDs (conductivity, temperature, and depth) sensors can reveal the general structure of a water column. Off the west Australian coast, turbulent mixing, e.g. by surface wind stress, and the presence of the LC produce a well-mixed layer at the surface. The well-mixed layer is deeper within the LC than it is onshore or farther offshore. The mixed-layer depth, which can be greater than 100 m, varies with the season and El Niño – southern oscillation events (Feng *et al.* 2003). Below the well-mixed layer, the thermocline usually descends to around 400-m depth,

Table 1

Characteristics of the water masses found at the 1000-m isobath along the west Australian coast.

Water mass	Temperature (°C)	Salinity	Dissolved oxygen (µM/L)
Tropical surface water (TSW)	22–24.5	34.7–35.1	200–220
South Indian central water (SICW)	12–22	35.1–35.9	220–245
Subantarctic mode water (SAMW)	8.5–12	34.6–35.1	245–255
Antarctic intermediate water (AAIW)	4.5–8.5	34.4–34.6	115–245
North-west Indian intermediate (NWII) water	5.5–6.5	~34.6	100–110
Circumpolar deep water (CDW)	2–3.8	34.57–34.75	120–200
Antarctic bottom water (AABW)	0.8–1.8	~34.71	~210

although sub-layers may exist in this depth range. The sea surface temperature cools in the austral winter and warms in the austral summer, with the deepest mixed-layer depths occurring in winter (Hamilton 1986; Feng *et al.* 2003).

Woo and Pattiaratchi (2008) identified five water mass types in the upper Indian Ocean (< 1000-m depth) along the west Australian coast (see Table 1), which corresponded with classical water masses of the Indian Ocean (Wyrski 1971; Warren 1981). Two other water masses—circumpolar deep water (CDW) and Antarctic bottom water (AABW)—were also present in the deeper waters. Woo and Pattiaratchi (2008) observed all these water masses in the vertical distribution of salinity and dissolved oxygen as interleaving layers of salinity and dissolved oxygen (Figures 11 and 12).

In order of increasing depth, these water masses were:

- (i) low salinity tropical surface water (TSW)
- (ii) high salinity south Indian central water (SICW)
- (iii) high oxygen subantarctic mode water (SAMW)
- (iv) low salinity Antarctic intermediate water (AAIW)
- (v) low oxygen north-west Indian intermediate (NWII) water
- (vi) low oxygen upper circumpolar deep water (UCDW)
- (vii) high salinity lower circumpolar deep water (LCDW)
- (viii) cold (< 2 °C), high oxygen Antarctic bottom water (AABW).

Temperature, salinity and dissolved oxygen were measured to locate the above water masses and their positions relative to each other along the whole coast from North West Cape (21° S) to Cape Leeuwin (35° S) (Figure 12). In the following sections, we summarise the characteristics of each of the above water masses.

Tropical surface water (TSW)—salinity minimum

A layer of low salinity (< 35.1), warm (> 22°C) tropical water found in the surface water in the northern region between North West Cape and the Abrolhos Islands), corresponded with the temperature/salinity characteristics of the Leeuwin Current water. This water mass was derived from the Australasian Mediterranean water, a tropical water mass with origins in the Pacific Ocean central water and formed during transit through the Indonesian archipelago (Tomczak & Godfrey, 1994). At the North West Cape (21 °S), the northern extent of the study region, this water mass extended to 180 m and exhibited a surface salinity of less than 34.9 (Figure 12). With the southward passage of the Leeuwin Current, the water mass shallowed and disappeared at ~26 °S. The salinity signature (which was < 35.1) disappeared because of the entrainment of cooler, saltier south Indian central water (see below) from offshore due to eddy activity and geostrophic inflow (Woo *et al.*, 2006b).

South Indian central water (SICW)—salinity maximum

South Indian central water (SICW) was identified here as a salinity maximum layer (35.1–35.9). Along the 1000-m bathymetric contour, shipborne ADCP (acoustic Doppler current profiler) data revealed the SICW's core moving northward at a maximum speed of 0.3 ms⁻¹ along the 26.8 density (σ_t) level. However, near the shelf break this same water mass was part of the Leeuwin Current flowing southwards (Woo *et al.*, 2006b). Here, ADCP data indicated that the Leeuwin Current extended up to 300-m water depth, which was the total depth of the SICW (Figure 12). SICW had a temperature range of 12–22°C and was associated with weak minima of dissolved nitrate, silica, and phosphate. South of 29.0 °S, SICW was found at the surface. But northward of 29.0 °S, the salinity maximum gradually subducted beneath TSW, reaching a depth of 245 m at 21.5°S.

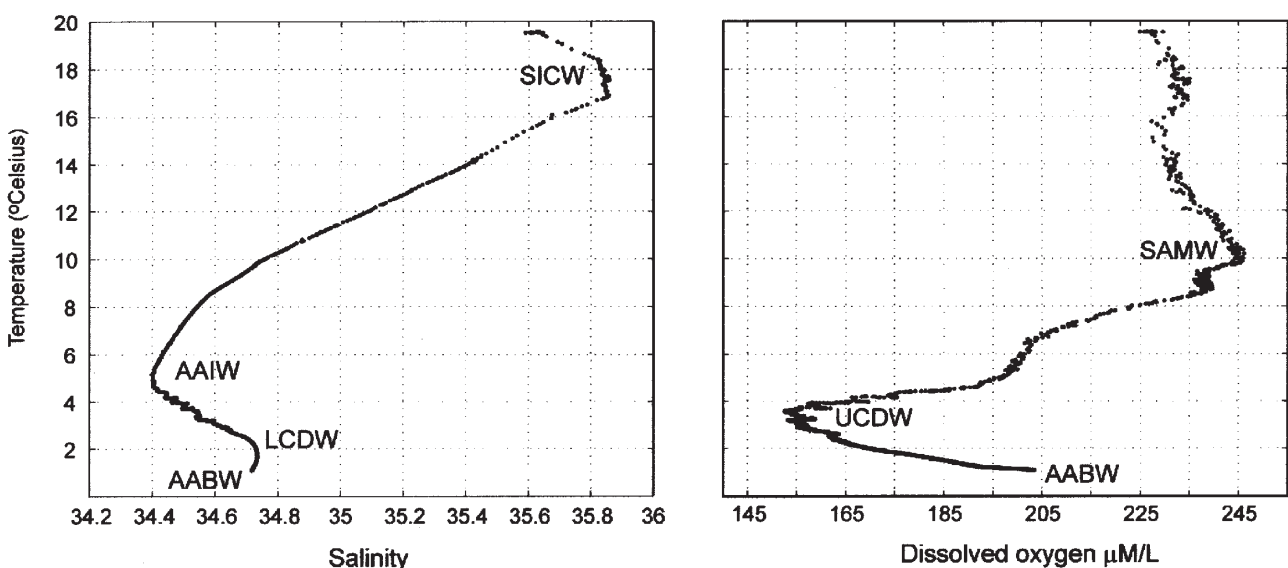


Figure 11. The temperature–salinity and temperature – dissolved oxygen diagrams for the Perth Basin showing the water masses off the west Australian coast. Station location is shown on Figure 2.

Subantarctic mode water (SAMW)—oxygen maximum

Beneath the south Indian central water (SICW), a water mass with high dissolved oxygen concentrations of 245–255 $\mu\text{M/L}$ was identified as subantarctic mode water (SAMW) whose core occurred at 400–510 m (Figure 12). SAMW consisted of water with a temperature range of 8.5°–12°C and salinity range of 34.6–35.1. SAMW is formed by deep winter convection at 40°–50°S in the zone between the subtropical convergence and the Subantarctic Front to the south of Australia (Wong, 2005). As SAMW is formed by deep convection rather than subduction, newly formed SAMW penetrates to a greater depth than the newly subducted SICW (thus, is comparatively better ventilated) and then moves northward from its formation region. Due to its high oxygen content, the SAMW plays an important role in ventilating the lower thermocline of the southern hemisphere subtropical gyres (McCartney, 1982). High oxygen content found in the core of the LU shows that the LU comprises of SAMW (Figure 4).

Antarctic intermediate water (AAIW)—salinity minimum

Below the SAMW, a salinity minimum (34.4–34.6) was observed, indicating the presence of Antarctic intermediate water (AAIW) along the coast (Figure 12).

The water was cold (4.5°–8°C) and the position of its core became shallower northward (the core depth was 875 m at 27.5°S and 520 m at 21.5°S). It has been reported the AAIW extends northward from the Antarctic Polar Front to latitudes 10°–15°S, and is thought to flow more slowly than the oxygen maximum layer above it (Warren, 1981).

Northwest Indian intermediate (NWII) water—oxygen minimum

An oxygen minimum signature of < 110 $\mu\text{M/L}$ in the northern region (21.3°–24.5°S) indicated the presence of northwest Indian intermediate (NWII) water immediately beneath the AAIW (Figure 12). This water mass originated from the Red Sea and Persian Gulf outflows. Occupying depths of 800–1175 m, the temperature of the NWII water was < 5°C and its salinity ranged between 34.55 and 34.65. NWII water was associated with maxima of dissolved nitrate, silica and phosphate.

Upper circumpolar deep water (UCDW) and lower circumpolar deep water (LCDW)

In the southern region (between the Abrolhos Islands and Cape Leeuwin), a water mass with similar characteristics to NWII water was found below the AAIW

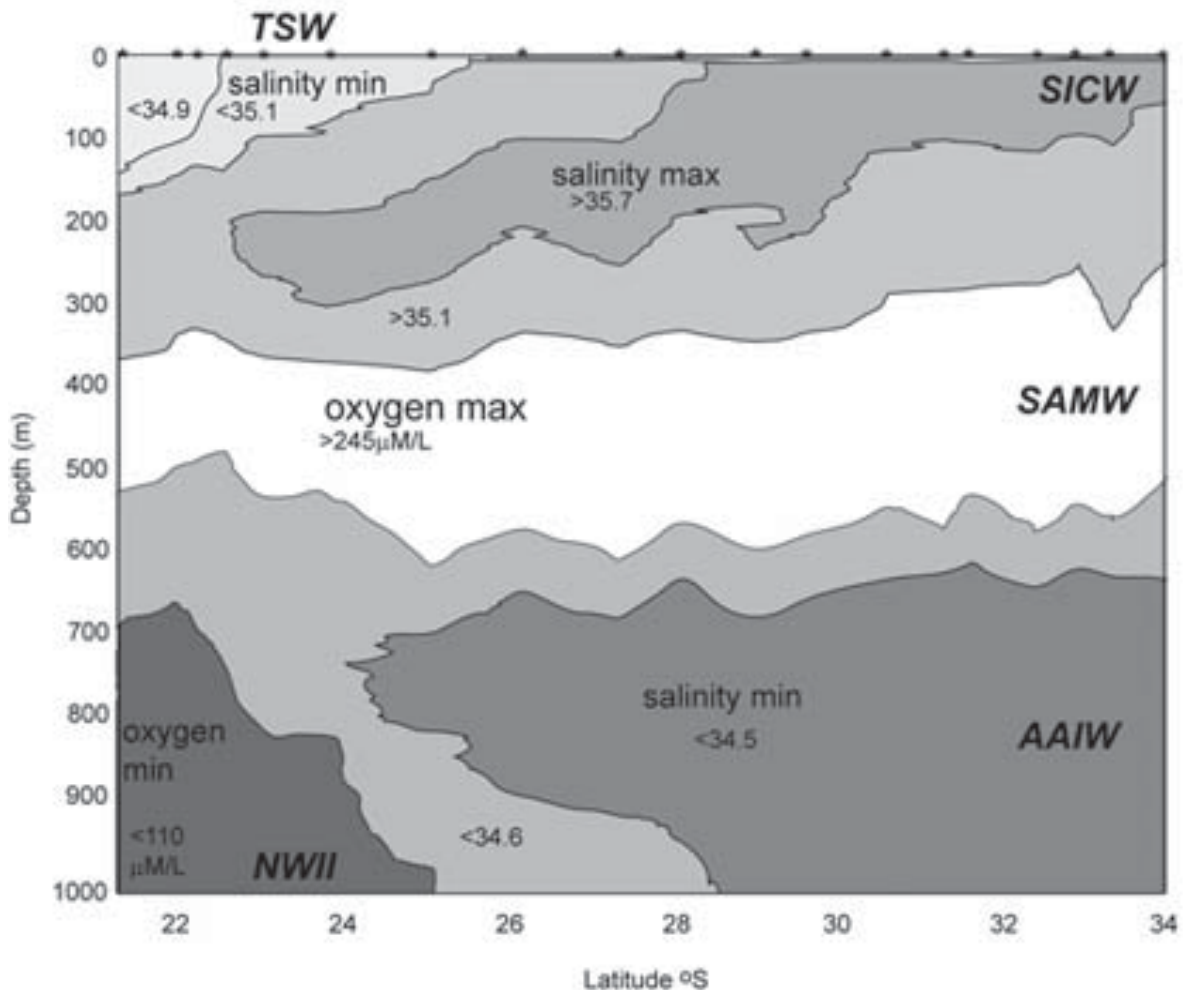


Figure 12. The main water masses observed at a section along the 1000-m isobath, parallel to the west Australian coast (modified from Woo & Pattiaratchi 2008).

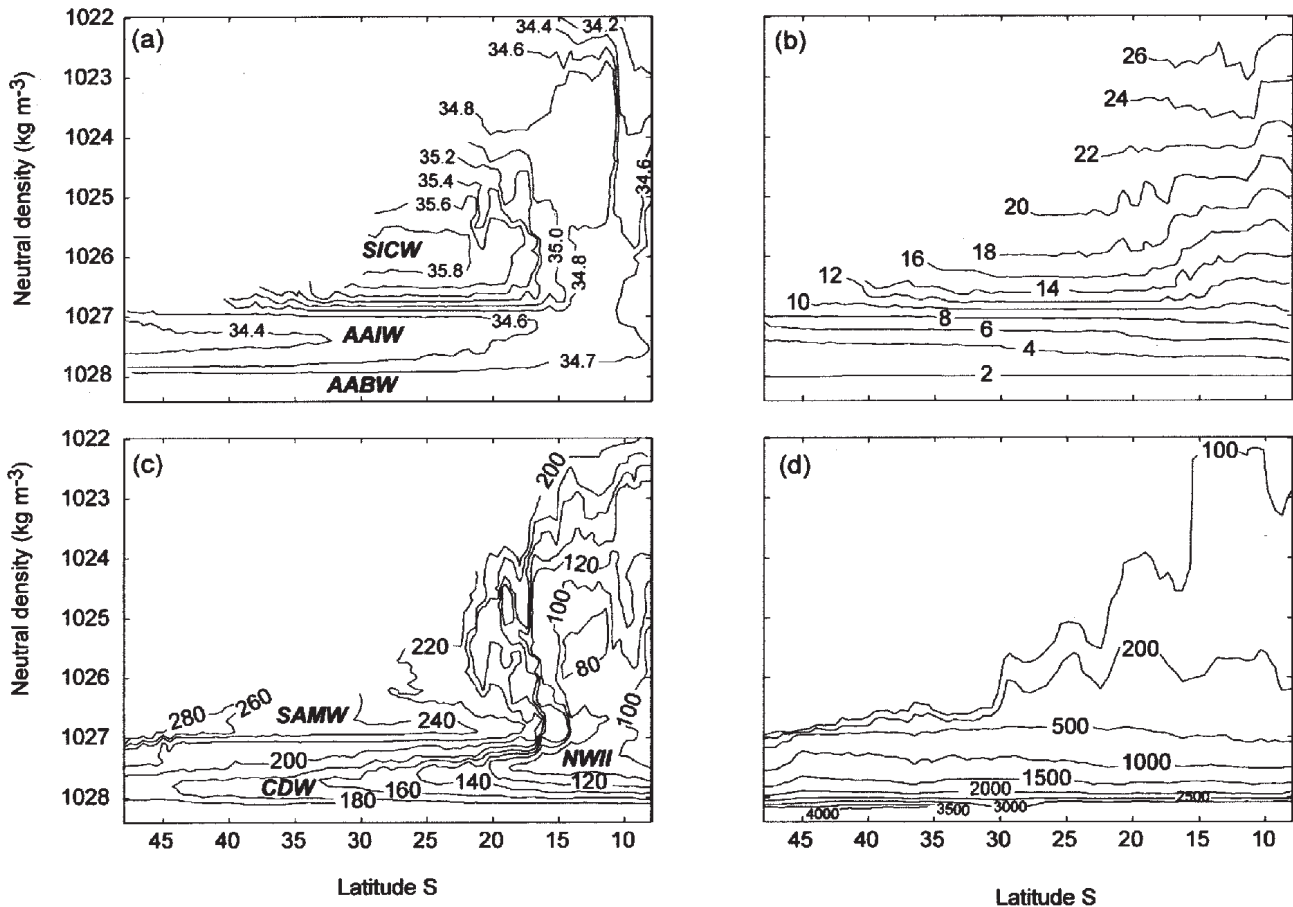


Figure 13. The isopleths of salinity (a), temperature (in degrees Celsius) (b), dissolved oxygen concentration (in M/L) (c), and depth (in metres) (d) plotted against neutral density (kg/m^3). The data for the region south of 35°S were obtained from voyage FR10/1994 (along 120°E), and the data for the region north of 34°S were obtained from voyage FR09/2000 (along 95°E).

and identified as circumpolar Deep Water (CDW). The CDW could be separated into two distinct water masses: lower circumpolar deep water (LCDW) and upper circumpolar deep water (UCDW) (Figure 11).

Lower Circumpolar Deep Water (LCDW) directly overlaid AABW (see below). It was characterised by a salinity maximum reaching 34.75 in the south and 34.72 in the north (Figure 13a). This water mass has also been referred to as Indian deep water (IDW) and upper deep water (Tomczak & Godfrey 1994). The high salinity content in LCDW is formed by North Atlantic Deep Water (NADW) being injected into the Antarctic Circumpolar Current (ACC) (Whitworth *et al.* 1998; Fieuz *et al.* 2005), and then gradually getting modified along its course through constant mixing with deep waters during its eastward journey in the ACC (Tomczak & Lieftrink 2005). LCDW moved along the 28.07kg/m^3 neutral density surface. Its oxygen content decreased from $>200\mu\text{M/L}$ in the south to $170\mu\text{M/L}$ in the north, thus indicating northward motion (Figure 13c). LCDW maintained potential temperature of around 1.5°C in a depth range of $2600\text{--}3100\text{m}$ (Figure 13b).

Upper circumpolar deep water (UCDW), which occurred just beneath Antarctic intermediate water

(AAIW), was characterised by an oxygen minimum (Tomczak & Lieftrink 2005). UCDW was observed flowing at depths of around 1550m on a neutral density surface of 27.8kg/m^3 , with its oxygen concentration decreasing from $180\mu\text{M/L}$ in the south to $120\mu\text{M/L}$ in the north (Figure 13c). Potential temperatures and salinities both increased northward, from $2.6^\circ\text{C}/34.57$ to $3.6^\circ\text{C}/34.75$ respectively.

Antarctic bottom water (AABW)

Antarctic bottom water (AABW) is one of the densest water mass found in the World Ocean (Tomczak & Lieftrink 2005). AABW flows onto the West Australian Basin, forming a western boundary current along the Ninety East Ridge (Tomczak & Godfrey 1994). As the area of the 28.2kg/m^3 neutral density surface is limited to the southern part of the Perth Basin, AABW must upwell (Sloyan 2006). Indeed, the continuity of AABW into the West Australian Basin was clearly detected in deep CTD records ($>4000\text{m}$ depth) taken in the West Australian Basin. Across 8°S where data was sampled down to 5000m (28.18kg/m^3 neutral density), the bottom water exhibited a salinity of 34.71 , potential temperature of 0.6°C and dissolved oxygen concentration of $210\mu\text{M/L}$, which is typical of AABW in these basins.

Recent observations of the Leeuwin current system

The CTD data of the Leeuwin current system obtained during the Leeuwin Current Interdisciplinary Experiment (1987–1988) (Church *et al.* 1989; Smith *et al.* 1991) supplemented Rochford's (1969) and Thompson's (1984) studies of the LC. Cresswell and Peterson (1993) also used CTD and ADCP measurements to study the LC off south-west Australia. Recent studies of the LC include those of Fieux *et al.* (2005) and Woo *et al.* (2006b). Woo *et al.* (2006b) used the research vessel ORV *Franklin* (voyage no. FR10/2000) to study the oceanographic processes along the continental shelf and slope between North West Cape and the Abrolhos Islands (referred to here as the northern region) in November 2000. Twomey *et al.* (2007) used the RV *Southern Surveyor* (voyage no. SS06/2003) to study the phytoplankton–nitrogen dynamics across the continental shelf between the Abrolhos Islands and Cape Leeuwin (referred to here as the southern region) in November 2003. Here we summarise the results obtained from both regions.

The two voyages took place in the early austral summer (October/November) of 2000 and 2003. Between 13 and 27 November 2000, eleven cross-shelf transects were obtained between 21 and 28° S in the northern

region (Figure 2); between 24 October and 9 November 2003, fourteen cross-shelf transects were obtained between 28 and 35° S in the southern region (Figure 2). The instruments deployed included a Neil Brown CTD recorder (FR10/2000) and a Sea-Bird CTD sensor (SS06/2003), each with a 24 × 5-L bottle on a Niskin rosette (for calibration and water sampling), a 150-kHz RDI acoustic Doppler current profiler (ADCP) linked to the global positioning system, a Turner Designs fluorometer, a near-surface thermosalinograph, and meteorological sensors. On both voyages, the cross-shelf stations extended from 50 to 1000-m water depths. Depending on the continental shelf width, 10–15 stations were occupied at the 50-m, 100-m, 150-m, 200-m, 250-m, 300-m, 500-m, 750-m, and 1000-m depth contours. Note that these studies occurred in the late spring and early summer when the LC is usually weaker.

North West Cape to the Abrolhos Islands

Woo *et al.* (2006b) studied the region between North West Cape and the Abrolhos Islands and found it comprised four different water masses (Figures 14 and 15). Offshore eddies, wind stress, varying shelf widths, the coastal topography, and outflow from the hypersaline Shark Bay all affected this complex current system. Hanson *et al.* (2005b) also studied this region off the west

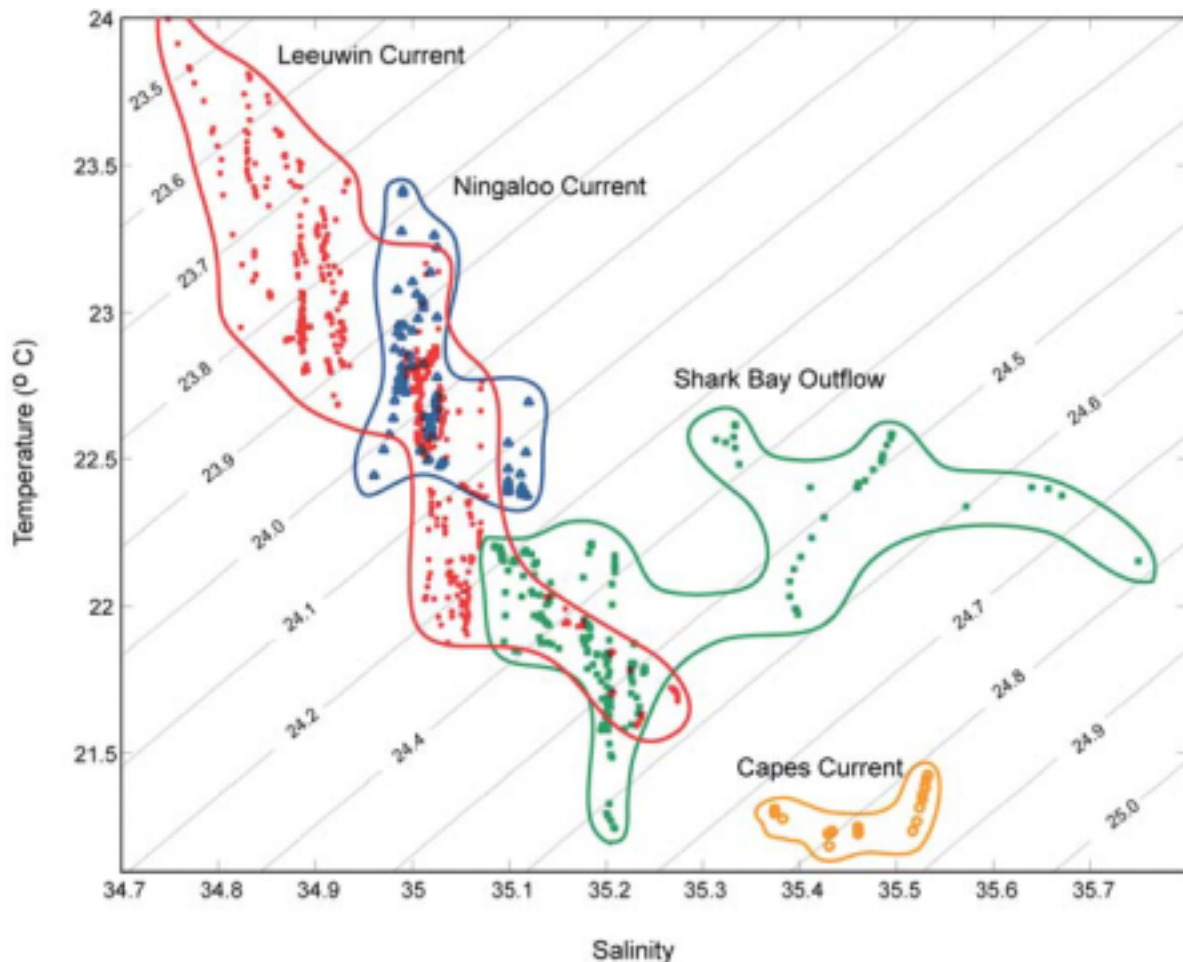


Figure 14. The temperature–salinity diagram of the surface water layer (top 100 m) from the coast to the 1000-m isobath in the northern region of the study area showing the presence of four different water masses (modified from Woo *et al.* 2006b).

Australian coast; however, they focused on the phytoplankton response to small-scale upwelling.

The LC transported warm, low salinity water poleward along the 200-m isobath. In the north, the LC water was warm (24.7 °C) and had a low salinity (34.6). As the current moved south, the geostrophic inflow of offshore waters cooled the LC water to 21.9 °C and increased its salinity to 35.2 (Figure 14).

The width and depth of the current also changed in response to the changing bottom topography and the coastline orientation. In the northern region, the narrow shelf and steep slope strengthened the current (recorded velocity of $\sim 0.75 \text{ ms}^{-1}$) and pushed it deep into the water column. In contrast, the current decelerated to $\sim 0.2\text{--}0.4 \text{ ms}^{-1}$ as it flowed past the wide continental shelf offshore Shark Bay and then accelerated in the southern region as it flowed along the steep continental slope. Changes in the shelf width at Point Cloates also split the northward moving Ningaloo current (Figure 15).

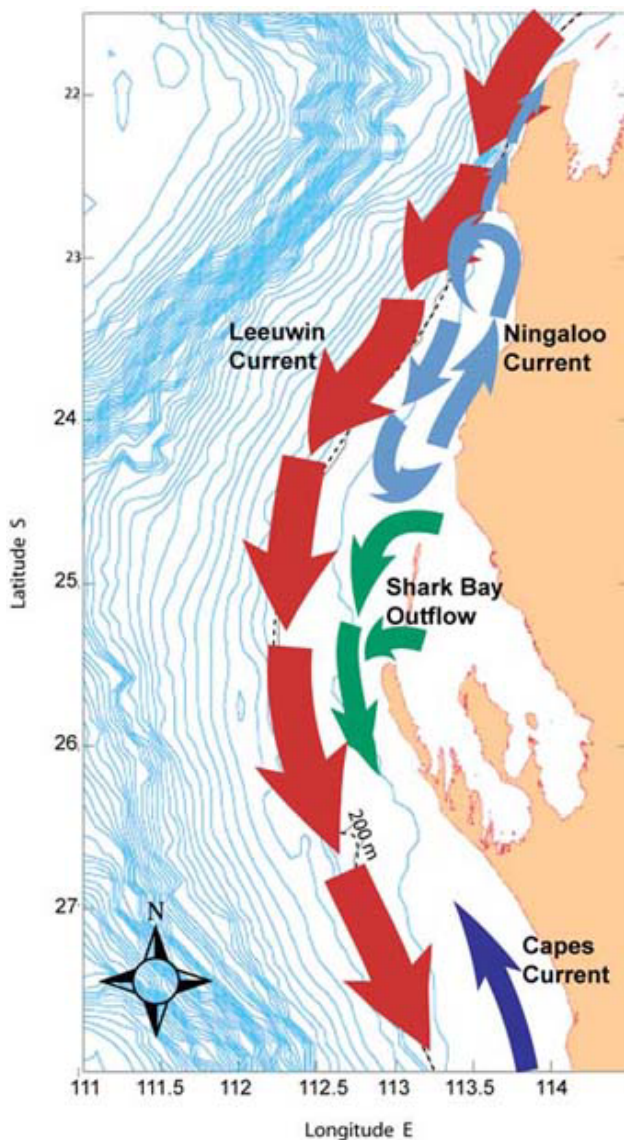


Figure 15. Schematic of the surface circulation in the northern region of the study area based on field data collected aboard the ORV *Franklin* (from Woo *et al.* 2006b).

Downwelling events were usually associated with the current. The Ningaloo current was confined to the north Gascoyne shelf within 35 km of the coast. Although upwelling was detected in the northern region, adjacent to the Ningaloo coral reef, the water properties suggested the LC water was recirculated from the south (Figure 14). In the continental shelf region to the west of the main bay entrances, the high salinity outflow water mixed with the shelf waters. The Capes current, a wind-driven current originating from the south of the study region, was identified as a cool, high salinity water mass flowing north.

The Abrolhos Islands to Cape Leeuwin

The voyage was completed over a period of 17 days and the CTD transects (Figure 2) were undertaken from north to south. At the beginning of the voyage, the winds were weak and gradually increased to speeds $> 8 \text{ ms}^{-1}$ and from a southerly direction (see Figure 5d; Hanson *et al.*, 2005b). Thus, the northerly transects were undertaken under low wind conditions whilst the southerly transects were undertaken during strong southerly (upwelling favourable) winds.

The cross-shelf CTD and ADCP transects provided detailed information on the LC's cross-sectional structure and the changes the LC underwent as the LC moved through the study region. For example, Figure 16 shows that at transect 2, the LC core at the surface was warmer (recorded temperature of $\sim 20 \text{ }^\circ\text{C}$) than the surrounding water, had a low salinity (~ 35.55), flowed poleward with speeds of $> 0.60 \text{ ms}^{-1}$, and extended to a depth of $\sim 250 \text{ m}$ (the ADCP's maximum depth limit). The steep continental slope and the changes in the shoreline orientation caused the LC to accelerate in this region (Woo *et al.* 2006b; Meuleners *et al.* 2007). On the continental shelf, the current flowed north but was weak (recorded speed of $\sim 0.10 \text{ ms}^{-1}$) because of the weak winds. The temperature and salinity isopleths beneath the LC were also depressed, which suggested downwelling had occurred.

Figure 17 shows that at transect 12, the LC core was warm but had a higher salinity content than the LC core at transect 2. The LC's surface salinity had increased to > 35.75 ; its temperature had decreased to $18 \text{ }^\circ\text{C}$; its speed had decreased to $\sim 0.20 \text{ ms}^{-1}$; and its core was located farther offshore. Upwelling had occurred on the continental shelf, and strong, northward currents ($> 0.30 \text{ ms}^{-1}$) indicated the presence of the Capes current. These findings agreed with Gersbach *et al.*'s (1999) observations that southerly winds with speeds $> 8 \text{ ms}^{-1}$ overcame the alongshore pressure gradient, pushed the surface waters and the LC farther offshore, and upwelled cold water onto the continental shelf (Figure 7).

Comparison of the northern and southern regions

The ORV *Franklin* and RV *Southern Surveyor* CTD data obtained at the 1000-m depth contour were used to build a pseudo-CTD transect line (Figure 18). Note that the transects for both voyages were obtained at around the same time of year (October/November) and thus showed an interannual variability. The southernmost transect of the ORV *Franklin* voyage was also used as the northernmost transect of the RV *Southern Surveyor*

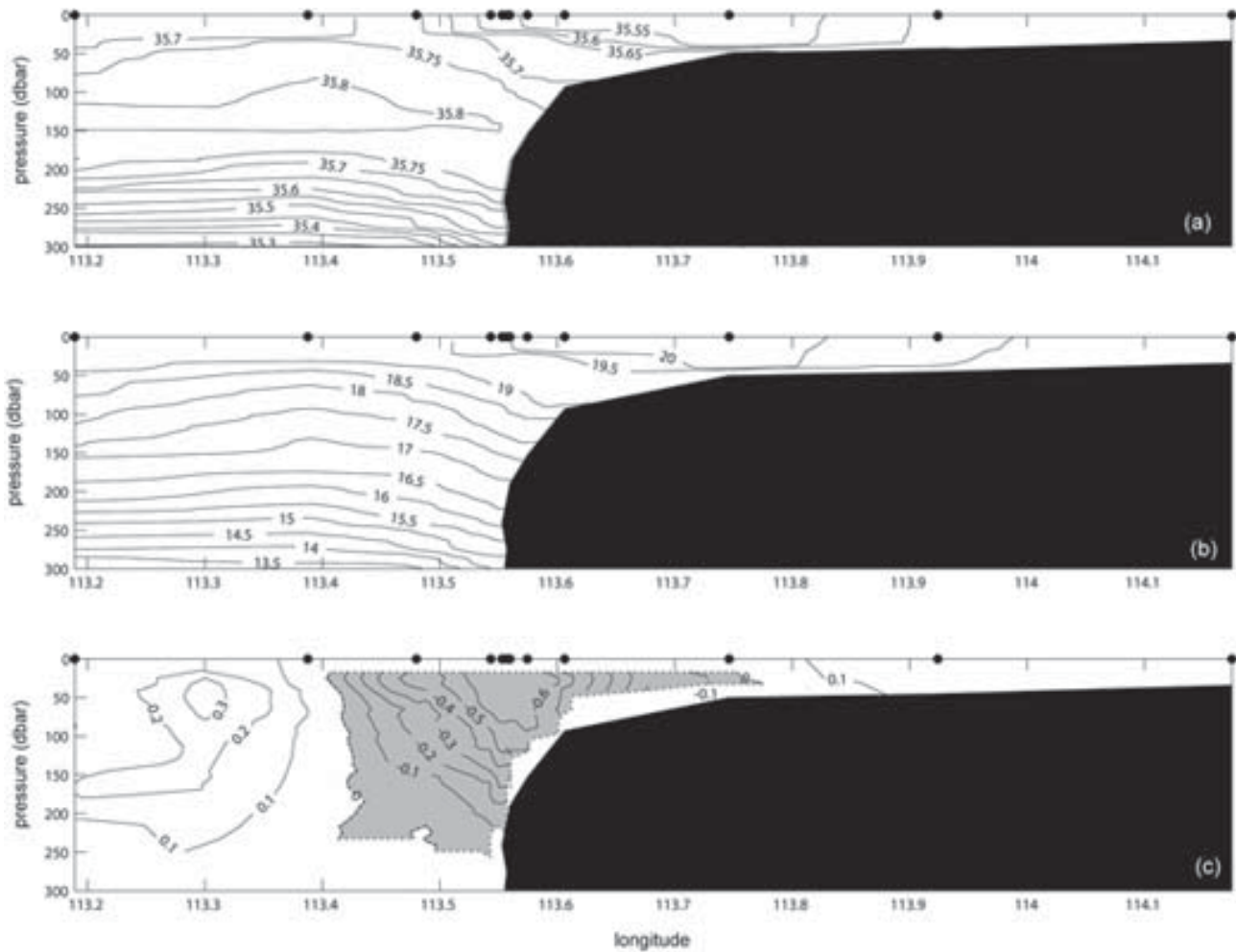


Figure 16. Transect 2 cross-sections (to 300-m depth) of salinity (a), temperature (b), and alongshore velocity (c) obtained with the ADCP. The shaded region in (c) indicates a poleward flow.

voyage. The data obtained at the 1000-m depth contour (Figure 18) showed the surface water temperature had decreased by ~ 1 °C (from 21 to 20 °C) and the salinity had increased by 0.3 (from 35.3 to 35.6) between November 2000 and October/November 2003. These changes in the surface water were most likely due to the LC weakening between 2000, a La Niña year, and 2003, and supported Feng *et al.*'s (2003) findings that the LC was stronger during La Niña events than it was during El Niño events.

Woo *et al.* (2006b) found that mixing changed the LC's temperature and salinity as the LC moved south—a process known as 'ageing'. The LC was warm (recorded temperature of 24 °C) with a salinity of 34.7 at the northern end of the transect (21° S). At the southern end of the transect (35° S), the water had cooled to 17.5 °C and its salinity had increased to 35.7 (Figure 18). Evaporation and atmospheric cooling would have contributed to these changes in the LC's water properties; however, the LC 'ageing' was mainly due to the presence of an onshore geostrophic flow from the central Indian Ocean with a maximum volume transport of 4 Sv

(derived from cool, salty SICW) and the LC mixing with water from farther offshore (Smith *et al.* 1991; Woo *et al.* 2006b).

A subsurface salinity maximum recorded in the northern region (Figures 11–13), which reached the water surface south of 29.5° S (Figures 12 and 18), revealed the presence of SICW. The transition of the salinity maximum from the subsurface to the surface was rapid: the 35.7 salinity contour rose from ~ 150 -m depth to the surface between 28 and 29.5° S. The cross-shore salinity transects 2 and 12 also showed the change in the LC between the northern and southern regions: at transect 2 (Figure 16), the subsurface core (at the 35.8-contour) had a high salinity, whereas at transect 12 (Figure 17), the salinity core was absent and the surface salinity was 35.75.

Field data obtained from the northern region revealed the presence of four surface water masses: the Leeuwin current, the Ningaloo current, the Capes current, and Shark Bay outflow (Figure 14). Field data obtained from the southern region (Figures 19 and 20) also showed the presence of four surface water masses: the Leeuwin

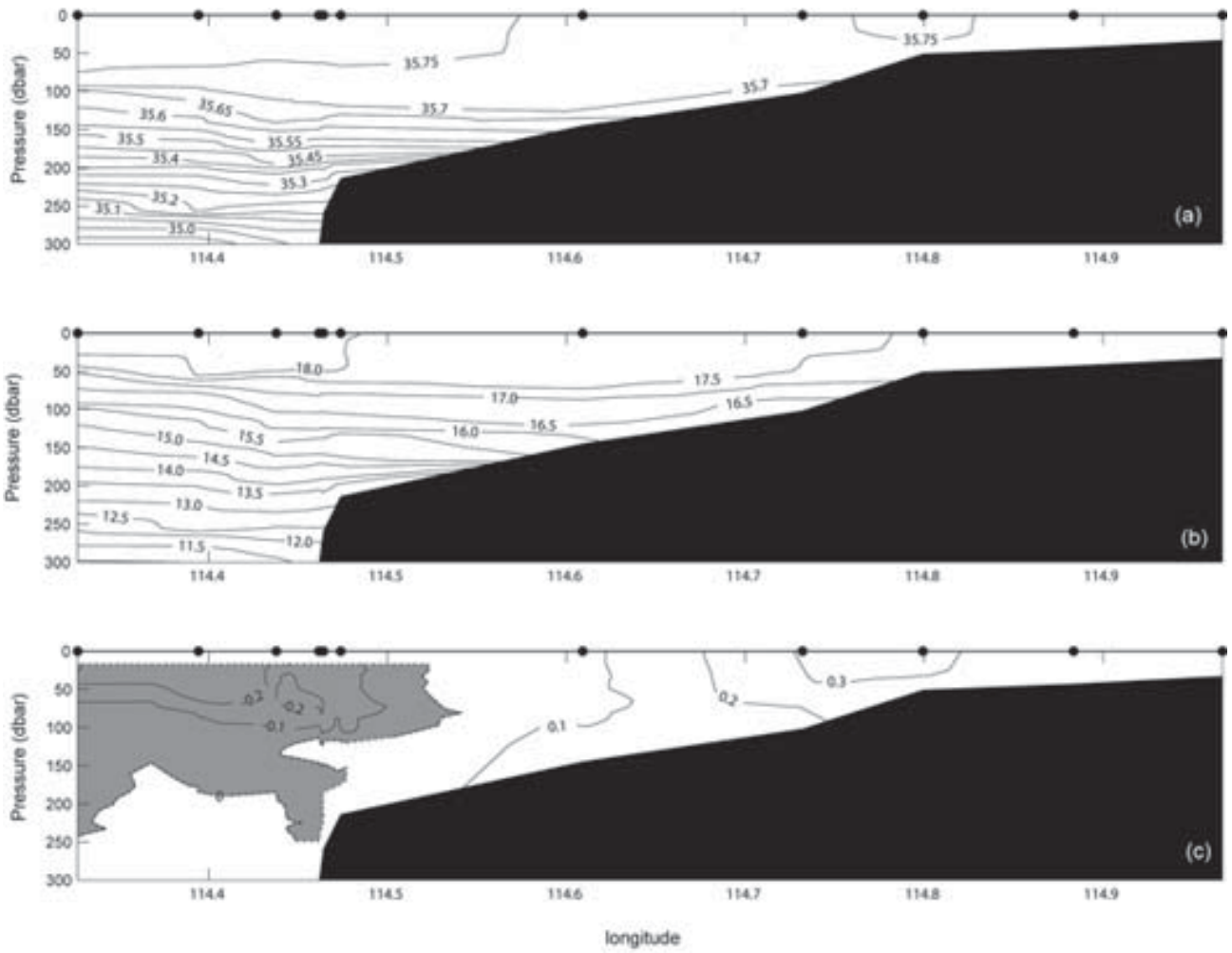


Figure 17. Transect 12 cross-sections (to 300-m depth) of salinity (a), temperature (b), and alongshore velocity (c) obtained with the ADCP. The shaded region in (c) indicates a poleward flow.

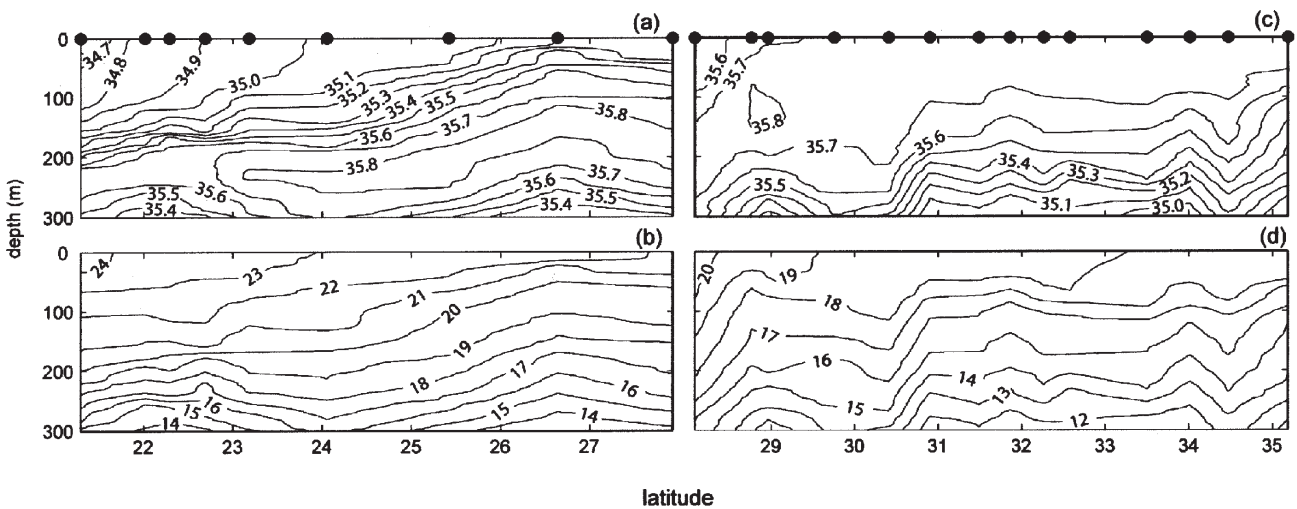


Figure 18. The alongshore transects of salinity (a) and temperature (in degrees Celsius) (b) at the 1000-m isobath for the northern region of the study area, and the alongshore transects of salinity (c) and temperature (in degrees Celsius) (d) at the 1000-m isobath for the southern region.

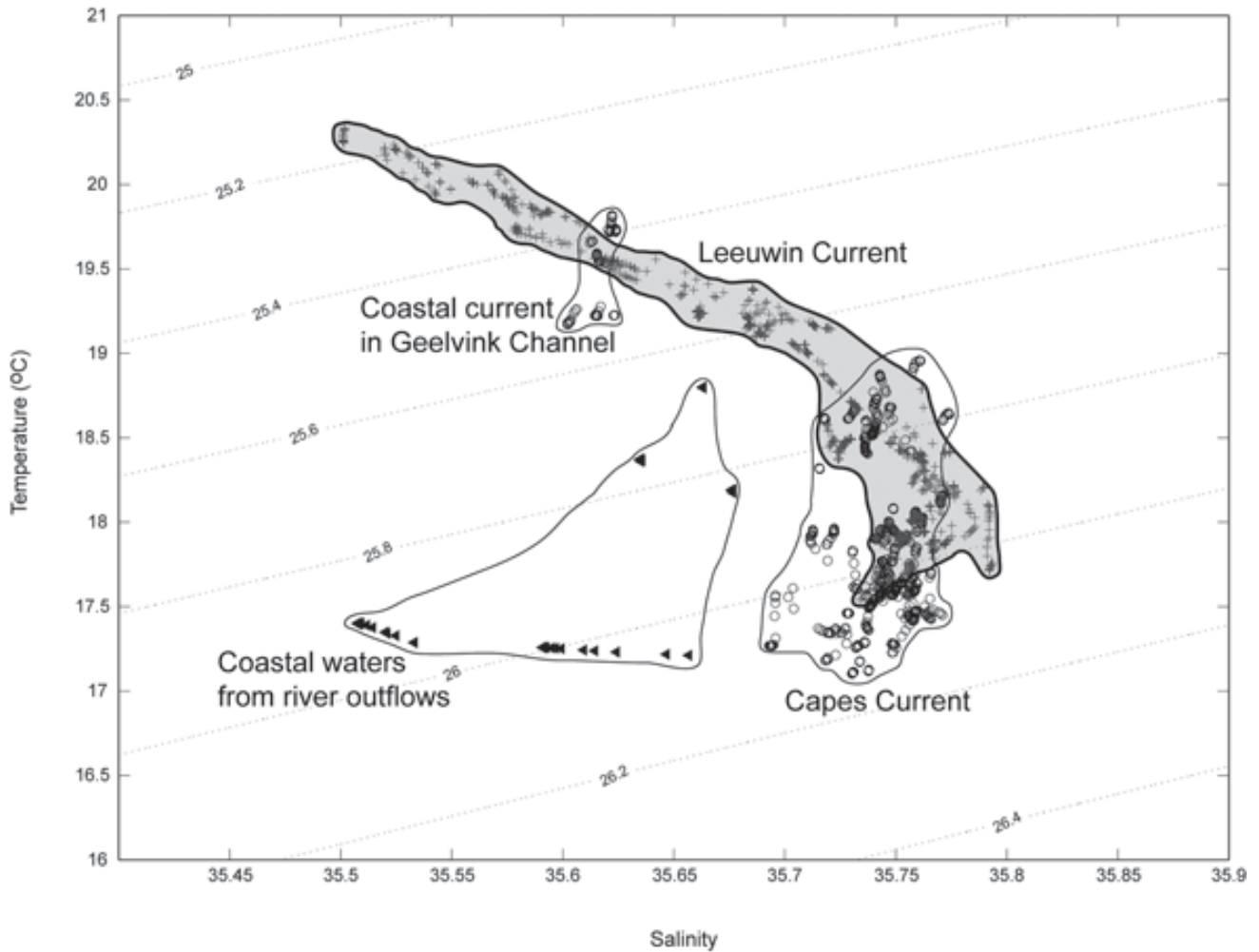


Figure 19. The temperature–salinity diagram of the surface water layer (top 100 m) from the coast to the 1000-m isobath in the southern region of the study area showing the presence of four different water masses.

current, the Capes current, water from the Geelvink Channel, and coastal waters offshore the Perth region.

The Capes current was present on the continental shelf as a continuous current from Cape Leeuwin to Geraldton (Figure 20), a distance of 750 km, and consisted of cold (17–19 °C), high salinity (35.68–35.78) water (Figure 20). The water from the Geelvink Channel to the north of Geraldton (Figure 20) overlapped with the LC, but was distinct from the Capes current (Figure 19). This water was most likely LC water that had moved onto the shelf and been changed by in situ processes. The SICW's high salinity core was located in deep water, beneath the source of the upwelling water, and thus did not introduce a salinity signature into the upwelling water. In contrast, the Capes current consisted of high salinity water because the SICW water was located at the surface.

The region offshore Perth received fresh water from estuarine and river systems such as the Swan, Peel–Harvey (Harvey and Murray rivers), and Leschenault (Capel and Brunswick rivers). The presence of cold, low salinity water at the shallow (< 50 m) stations closest to the coast showed the fresh water's effect on the coastal waters in late spring (Figure 19). Thus in a similar

manner to the high salinity discharge from Shark Bay influencing the waters offshore Shark Bay, the freshwater discharge from the estuarine and river systems in the southern region influenced the shallow continental shelf waters offshore Perth. The seasonal salinity cycle at the 30-m isobath to the north of Perth also showed minimum values in September and maximum values in February, which suggested the coastal waters observed offshore Perth in the southern region were most likely a seasonal feature (Zaker *et al.* 2007).

Figure 20 shows the main features of the surface currents and associated water masses present in the southern region between October and November 2003. These recorded values reflected typical summer conditions, especially in the southern region, where strong, consistent southerly winds were experienced; however, the low salinity coastal waters were most likely absent.

The findings from the northern and southern regions can be summarised thus: the LC flowed from north to south along the 200-m isobath. Inshore of the LC, the Capes current flowed north, advecting cool, high salinity water from the south. The coastal waters offshore Perth received fresh water from estuarine and river systems,

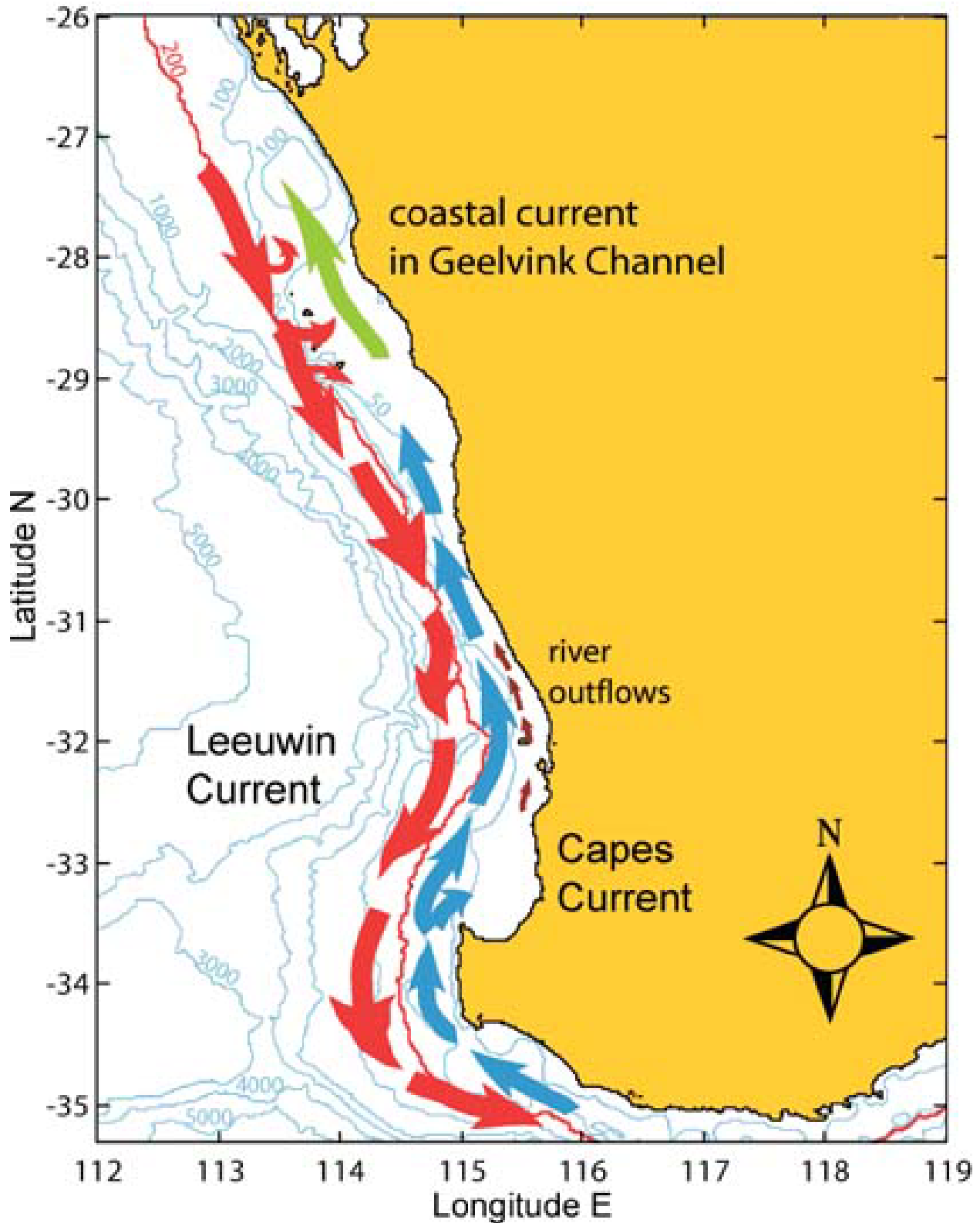


Figure 20. Schematic of the surface circulation in the southern region of the study area based on field data collected aboard the RV *Southern Surveyor*.

which lowered the salinity of the coastal waters, while localised upwelling produced a distinct water mass in the Geelvink Channel. Several water masses, distinguishable by their temperature and salinity

characteristics, were present and each had a unique biological identity with different primary production regimes and phytoplankton species composition (Hanson *et al.* 2005a; Twomey *et al.* 2007).

Acknowledgements: We thank the captains, crew, and staff of the RV Franklin and FRV Southern Surveyor for successfully executing cruises FR10/2000 and SS09/2003. We acknowledge Ruth Gongora-Mesas for her assistance in preparing the final manuscript.

References

- Akhir M F & Pattiaratchi C B 2006 Summer physical processes along the continental shelf and slope off southern Western Australia. *Proceedings of the Sixth International Symposium on Stratified Flows*. The University of Western Australia, Perth, 239–244.
- Andrews J C 1977 Eddy structure and the West Australian current. *Deep-Sea Research* 24: 1133–1148.
- Andrews J C 1983 Ring structure in the poleward boundary current off Western Australia in summer. *Australian Journal of Marine and Freshwater Research* 34: 547–561.
- Batteen M L & Rutherford M J 1990 Modeling studies of eddies in the Leeuwin current: the role of thermal forcing. *Journal of Physical Oceanography* 20: 1484–1520.
- Church J A, Cresswell G R & Godfrey J S 1989 The Leeuwin current. In: *Poleward Flows along Eastern Ocean Boundaries* (eds S J Neshyba, C N K Mooers, R L Smith & R T Barber). *Lecture Notes on Coastal and Estuarine Studies*, vol. 34. Springer-Verlag, New York, 230–252.
- Cirano M & Middleton J F 2004 Aspects of the mean wintertime circulation along Australia's southern shelves: Numerical studies. *Journal of Physical Oceanography* 34: 668–684.
- Cresswell G R 1996 The Leeuwin current near Rottnest Island, Western Australia. *Marine and Freshwater Research* 47: 483–487.
- Cresswell G R, Boland F M, Peterson J L & Wells G S 1989 Continental shelf currents near the Abrolhos Islands, Western Australia. *Australian Journal of Marine and Freshwater Research* 40: 113–128.
- Cresswell G R & Golding T J 1980 Observations of a south-flowing current in the southeastern Indian Ocean. *Deep-Sea Research Part A: Oceanographic Research Papers* 27: 449–466.
- Cresswell G R & Peterson J L 1993 The Leeuwin current south of Western Australia. *Australian Journal of Marine and Freshwater Research* 44: 285–303.
- Eliot I G & Clarke D J 1986 Minor storm impact on the beachface of a sheltered sandy beach. *Marine Geology* 73: 61–83.
- Fang F & Morrow R 2003 Evolution, movement and decay of warm-core Leeuwin current eddies. *Deep-Sea Research Part II: Topical Studies in Oceanography* 50: 2245–2261.
- Feng M, Meyers G, Pearce A & Wijffels S 2003 Annual and interannual variations of the Leeuwin current at 32° S. *Journal of Geophysical Research* 108: 3355.
- Feng M, Wijffels S, Godfrey J S & Meyers G 2005 Do eddies play a role in the momentum balance of the Leeuwin current? *Journal of Physical Oceanography* 35: 964–975.
- Fioux M, Molcard R & Morrow R 2005 Water properties and transport of the Leeuwin current and eddies off Western Australia. *Deep-Sea Research Part I: Oceanographic Research Papers* 52: 1617–1635.
- Gentili J 1972 *Australian Climate Patterns*. Thomas Nelson, Melbourne.
- Gersbach G H, Pattiaratchi C B, Ivey G N & Cresswell G R 1999 Upwelling on the south-west coast of Australia—source of the Capes current? *Continental Shelf Research* 19: 363–400.
- Godfrey J S & Ridgway K R 1985 The large-scale environment of the poleward-flowing Leeuwin current, Western Australia: Longshore steric height gradients, wind stresses, and geostrophic flow. *Journal of Physical Oceanography* 15: 481–495.
- Godfrey J S, Vaudrey D J & Hahn, S D 1986 Observations of the shelf-edge current south of Australia, winter 1982. *Journal of Physical Oceanography* 16: 668–679.
- Hamilton L J 1986 Statistical features of the oceanographic area off south-western Australia, obtained from bathythermograph data. *Australian Journal of Marine and Freshwater Research* 37: 421–436.
- Hanson C E, Pattiaratchi C B & Waite A M 2005a Seasonal production regimes off south-western Australia: Influence of the Capes and Leeuwin currents on phytoplankton dynamics. *Marine and Freshwater Research* 56: 1011–1026.
- Hanson C E, Pattiaratchi C B & Waite A M 2005b Sporadic upwelling on a downwelling coast: Phytoplankton responses to spatially variable nutrient dynamics off the Gascoyne region of Western Australia. *Continental Shelf Research* 25: 1561–1582.
- Hickey B M 1995 Coastal submarine canyons. *Topographic Effects in the Ocean: Proceedings of the Eighth 'Aha Huliko'a Hawaiian Winter Workshop*. School of Ocean and Earth Science and Technology, University of Hawaii, 95–110.
- James N P, Collins L B, Bone Y & Hallock P 1999 Subtropical carbonates in a temperate realm: Modern sediments on the southwest Australian shelf. *Journal of Sedimentary Research* 69: 1297–1321.
- Keper T D & Smith R K 1992 A simple model of the Australian west coast trough. *Monthly Weather Review* 120: 2042–2055.
- Lemm A J, Hegge B J & Masselink G 1999 Offshore wave climate, Perth (Western Australia), 1994–96. *Marine and Freshwater Research* 50: 95–102.
- Masselink G & Pattiaratchi C B 2001 Characteristics of the sea breeze system in Perth, Western Australia, and its effect on the nearshore wave climate. *Journal of Coastal Research* 17: 173–187.
- McCartney M S 1982 The subtropical recirculation of mode waters. *Journal of Marine Research* 40(suppl.): 427–464.
- Meuleners M J, Pattiaratchi C B & Ivey G N 2007 Numerical modelling of the mean flow characteristics of the Leeuwin current system. *Deep-Sea Research Part II: Topical Studies in Oceanography* 54: 837–858.
- Middleton J F & Bye J A T 2007 A review of the shelf-slope circulation along Australia's southern shelves: Cape Leeuwin to Portland. *Progress in Oceanography* 75: 1–41.
- Morrow R, Fang F, Fioux M & Molcard R 2003 Anatomy of three warm-core Leeuwin current eddies. *Deep-Sea Research Part II: Topical Studies in Oceanography* 50: 2229–2243.
- Nahas E L, Pattiaratchi C B & Ivey G N 2005 Processes controlling the position of frontal systems in Shark Bay, Western Australia. *Estuarine, Coastal and Shelf Science* 65: 463–474.
- Pattiaratchi C B & Buchan S J 1991 Implications of long-term climate change for the Leeuwin current. *Journal of the Royal Society of Western Australia* 74: 133–140.
- Pattiaratchi C B, Hegge B, Gould J & Eliot I 1997 Impact of sea-breeze activity on nearshore and foreshore processes in southwestern Australia. *Continental Shelf Research* 17: 1539–1560.
- Pearce A F 1991 Eastern boundary currents of the Southern Hemisphere. *Journal of the Royal Society of Western Australia* 74: 35–45.
- Pearce A F & Pattiaratchi C B 1999 The Capes current: A summer countercurrent flowing past Cape Leeuwin and Cape Naturaliste, Western Australia. *Continental Shelf Research* 19: 401–420.
- Pearce A F & Pattiaratchi C B 1997 Applications of satellite remote sensing to the marine environment in Western Australia. *Journal of the Royal Society of Western Australia* 80: 1–14.
- Pearce A F & Walker D I (eds) 1991 *The Leeuwin current: An influence on the coastal climate and marine life of Western Australia*. *Journal of the Royal Society of Western Australia* 74: 1–140.
- Rennie S J, McCauley R D & Pattiaratchi C B 2006 Thermal structure above the Perth Canyon reveals Leeuwin current,

- undercurrent and weather influences and the potential for upwelling. *Marine and Freshwater Research* 57: 849–861.
- Rennie S J, Pattiaratchi C B & McCauley R D 2007 Eddy formation through the interaction between the Leeuwin current, Leeuwin undercurrent and topography. *Deep-Sea Research Part II: Topical Studies in Oceanography* 54: 818–836.
- Rennie, S J, Pattiaratchi C B & McCauley R 2009 Numerical simulation of the circulation within the Perth Submarine Canyon, Western Australia. *Continental Shelf Research*, doi:10.1016/j.csr.2009.04.010.
- Ridgway K R & Condie S A 2004 The 5500-km-long boundary flow off western and southern Australia. *Journal of Geophysical Research* 109, doi: 10.1029/2003JC001921.
- Rochford D J 1969 Seasonal interchange of high and low salinity surface waters off south-west Australia. CSIRO Division of Fisheries and Oceanography Technical Paper 29.
- Schott F A, McCreary J P, Jr, & Johnson G C 2001 The monsoon circulation of the Indian Ocean. *Progress in Oceanography* 51: 1–123.
- Schott G 1935 *Geographie des Indischen und Stillen Ozeans*. C Boysen, Hamburg.
- Sloyan B M 2006 Antarctic bottom and lower circumpolar deep water circulation in the eastern Indian Ocean. *Journal of Geophysical Research* 111, doi: 10.1029/2005JC003011.
- Smith R L, Huyer A, Godfrey J S & Church J A 1991 The Leeuwin current off Western Australia, 1986–1987. *Journal of Physical Oceanography* 21: 323–345.
- Taylor J G & Pearce A F 1999 Ningaloo Reef currents: Implications for coral spawn dispersal, zooplankton and whale shark abundance. *Journal of the Royal Society of Western Australia* 82: 57–65.
- Thompson R O R Y 1984 Observations of the Leeuwin current off Western Australia. *Journal of Physical Oceanography* 14: 623–628.
- Thompson R O R Y 1987 Continental shelf – scale model of the Leeuwin current. *Journal of Marine Research* 45: 813–827.
- Tomczak M & Godfrey J S 1994 *Regional Oceanography: An Introduction*. Pergamon Press, New York.
- Tomczak M & Lieftrink S 2005 Interannual variations of water mass volumes in the Southern Ocean. *Journal of Atmospheric and Oceanic Technology* 22: 31–42.
- Twomey L J, Waite A M, Pez V & Pattiaratchi C B 2007 Variability in nitrogen uptake and fixation in the oligotrophic waters off the south west coast of Australia. *Deep-Sea Research Part II: Topical Studies in Oceanography* 54: 925–942.
- Warren B A 1981 Trans-Indian hydrographic section at lat. 18° S: Property distributions and circulation in the south Indian Ocean. *Deep-Sea Research Part A: Oceanographic Research Papers* 28: 759–788.
- Weaver A J & Middleton J H 1989 On the dynamics of the Leeuwin current. *Journal of Physical Oceanography* 19: 626–648.
- Whitworth T, III, Orsi A H, Kim S-J, Nowlin W D, Jr, & Locarnini R A 1998 Water masses and mixing near the Antarctic slope front. In: *Ocean, Ice, and Atmosphere: Interactions at the Antarctic Continental Margin* (eds S Jacobs & R Weiss). Antarctic Research Series, vol. 75. American Geophysical Union, Washington, DC, 1–27.
- Wong A P S 2005 Subantarctic mode water and Antarctic intermediate water in the south Indian Ocean based on profiling float data 2000–2004. *Journal of Marine Research* 63: 789–812.
- Woo M & Pattiaratchi C B 2008 Hydrography and waters masses off the Western Australian coast. *Deep-Sea Research Part I: Oceanographic Research Papers* 55: 1090–1104.
- Woo M, Pattiaratchi C B & Schroeder W 2006a Dynamics of the Ningaloo current off Point Cloates, Western Australia. *Marine and Freshwater Research* 57: 291–301.
- Woo M, Pattiaratchi C B & Schroeder W 2006b Summer surface circulation along the Gascoyne continental shelf, Western Australia. *Continental Shelf Research* 26: 132–152.
- Wyrtki K 1971 *Oceanographic Atlas of the International Indian Ocean Expedition*. National Science Foundation, Washington, DC.
- Zaker N H, Imberger J & Pattiaratchi C B 2007 Dynamics of the coastal boundary layer off Perth, Western Australia. *Journal of Coastal Research* 23: 1112–1130.